EXHIBIT D

Supporting Watershed Studies

Calibration Report

Hydrologic modeling to support Hydromodification Management Plans:

Evaluation and calibration of the San Diego Hydrology Model to reference watersheds in San Diego

Trent Biggs[1], Anurag Mishra[2], Brian Haines[3], Luis de la Torre[1]

1. Department of Geography, San Diego State University, San Diego, CA, 92182
2. Aqua Terra Consultants, 2685 Marine Way, Suite 1314, Mountain View, CA-94043
3. ESA PWA, San Francisco, California 94108

Draft date: June 29, 2015
Revision date: July 24, 2015

Summary

The San Diego Hydrology Model (SDHM) was evaluated against observed discharge for two watersheds with minimal human disturbance: a small watershed (Wilson Creek Tributary, 0.6 mi^2) and a larger watershed (Guejito Creek, 22.4 mi^2). Initial runs used the recommended default parameters in two existing variations of the SDHM (SDHM2008, SDHM2011). SDHM2011 (hereafter SD11) was then calibrated to observed daily discharge, annual total discharge, and peak discharges at 2-, 5- and 10-year return intervals for both watersheds separately. Peak discharges (Qx) were calculated using both annual maximum series of 15-minute flow and the partial duration series of mean daily flow. Qx for the three return intervals were compared for the original SDHM2008 (hereafter SD08), original SD11, without and with channel infiltration, calibrated SD11, with and without channel infiltration, and regression equations from USGS and others. The model calibrated to the large watershed was also applied to the small watershed to test for the transferability of parameters across scales.

SD08 includes different parameters for trees, shrubs, grass, and dirt, while SD11 represents only grass, dirt, and gravel cover. Nonetheless, SD11 had much lower error than SD08. SD08 consistently overpredicted discharge at all exceedence probabilities for all watersheds, with errors in peak discharge up to >1500% (Q2). The default SD11 was relatively accurate for the large watershed (Guejito) with errors in peak discharges determined using partial duration series of +58% (Q2), +28% (Q5) and +20% (Q10), compared to -19% (Q2), -12% (Q5) and -6% (Q10) for the calibrated SD11 during the calibration period. The default SD11 performed better than the calibrated SD11 on the validation period, but the validation period was relatively dry and may not be a good test of the model's ability to predict channel-forming discharges.

SD11 was less accurate in the small watershed (Wilson) compared to the large watershed, with errors in the annual maximum series of 1200% (Q2), 198% (Q5) and 123% (Q10), compared to +25% (Q2), +5% (Q5) and +4% (Q10) for the calibrated model.

Consistent with other modeling efforts in San Diego County and a review of the SDHM, the calibrated SD11 model had significantly higher infiltration capacity, soil moisture storage capacity, and interflow than the uncalibrated SD11. The calibrated models produced a good fit between the modelled and observed flow duration curves (FDCs), though without channel infiltration, the fit at the smallest watershed (Wilson) relied on very high values of the groundwater loss coefficient (DEEPFR), suggesting that channel infiltration may be an important process in small watersheds. Including

channel infiltration in the calibrated model allowed decreasing DEEPFR to within the accepted range in BASINS Technical Note 6, and parameters for infiltration and lower zone soil moisture storage (LZSN) were more consistent with other literature values, though the errors in the predictions of daily and peak flows were similar or higher in the model with channel infiltration compared with the model without channel infiltration.

The predictions of peak discharge by the regression equations had lower error than the predictions from the uncalibrated SD11 for Q5 and Q10, but had higher error than SD11 for Q2. The error in prediction of peak discharges from the partial duration series decreased with return interval: Q2 was overall the most difficult to predict and Q10 the easiest to predict for all models.

Overall, the results suggest that:

1) SD11 predicts higher peak and annual discharge than is observed, particularly for the smallest watershed (0.6 mi^2). SD11 produces errors of less than 60% for peak flow from the partial duration series of mean daily flow for the large watershed, but has higher error for small watersheds (+1200% for Q2 and 123-198% for Q5 and Q10 from the annual maximum series).

2) High return interval flows (Q5, Q10) are predicted with less error than low return interval flow (Q2). Errors in SD11 at the small watershed were high for Q2 (+1200%) but relatively low for both the default parameter set for Q5 (+198) and Q10 (+123%) and for SD11 calibrated to discharge at the large watershed (error +19% Q5 and +47% Q10). We conclude that parameters from the model calibrated to the large watershed can be used for models of small watersheds with errors of <50% in Q5 and Q10, but with large errors in the annual water balance and baseflow.

3) The regression equations performed better than the uncalibrated SD11 in predicting the annual maximum flow series. The lowest errors in Qx predicted by SD11 were achieved for the partial duration series, which is not predicted by the USGS regressions due to the lack of sufficient discharge data at 15-minute resolution.

Introduction

The San Diego Hydrology Model (SDHM) is a regulatory tool used to estimate flow duration curves and floods of various recurrence intervals both pre- and post-development. The models support implementation of the Hydromodification regulations that are being developed and applied in San Diego County. In most cases, regulatory application is for small watersheds (< 25 mi^2), so there is a need to quantify the accuracy and uncertainty in model predictions at those small spatial scales.

Several versions of the SDHM are available. Two of these models, SD08 and SD11, were developed by two different consulting groups (Brown and Caldwell, and Clear Creek Solutions), though the documentation for both models was prepared by Clear Creek Solutions. Both SD08 and SD11 have been reviewed by a third party (Tetra Tech, 2011). The model parameters in both versions of the SDHM were derived from other models applied to watersheds in southern California, but most of those watersheds were large and had significant human activity, including a watershed with irrigated agriculture (Calleguas Creek in Ventura County) (AQUA TERRA, 2005) and Santa Monica Bay (Ackerman et al., 2005), whose model parameters were taken mostly from the Bay Area Hydrology Model (BAHM), which in turn was calibrated to watersheds in northern California , including one small (5.5 mi^2) watershed with mostly urban and suburban land cover (Castro Valley Creek in Santa Clara County near the city of San Jose) and a larger watershed (33.5 mi^2) that has rugged topography but was undeveloped at the time of calibration (Alameda Creek in Alameda County) (AQUA TERRA, 2006; Bicknell et al., 2006). Most of the model parameters in SDHM inherit their values from these calibration attempts in watersheds with mixed land cover, though there are recognized difficulties with applying models developed for mixed land cover to watersheds with predominantly natural land cover.

The application in Santa Monica Bay (Ackerman et al., 2005) includes a large undeveloped watershed (Malibu Creek, 272 km^2 at the point of validation), but the parameter values presented in Ackerman et al (2005) do not vary by land cover or soil type and so cannot be compared with other HSPF models, including SD11.

A review of the SDHM models confirmed that no validation of any version of the SDHM has been performed for any streams in San Diego County (Tetra Tech, 2011). HSPF has been calibrated to one large, partly urbanized watershed in San Diego County (Los Penasquitos, 41.2 mi^2) (Tetra Tech, 2010). HSPF has been implemented for a watershed with mixed natural and agricultural areas whose watershed boundary includes part of San Diego County (Santa Margarita River, 588 mi^2) (RBF Consulting, 2013), but the model was based on the South Orange County Hydrology Model (SOHM) (Clear Creek Solutions, 2012), neither of which has been calibrated or validated against observed discharge data. No validation or calibration of any HSPF model has been attempted for small watersheds (<25 mi^2) in San Diego County. In addition, based on available documentation, no version of any HSPF model, including BAHM, its descendants, the SDHM, or SOHM, has been validated for small watersheds with natural vegetation cover for any watershed in California, despite the importance of accuracy of runoff predictions from small watersheds for successful application of the models for HMP purposes.

The SDHM incorporates many hillslope hydrological processes, including interception, infiltration, near-surface soil storage, evapotranspiration, interflow, and loss to deep groundwater. SDHM2011 has an option to incorporate channel infiltration, also known as channel transmission losses. Such losses can comprise a large fraction of the runoff generated from hillslopes, including the San Jacinto River Basin in southern California (Guay, 2002) and channels on alluvial sediments in Baja California (Ponce et al., 1999). Channel infiltration is most important along mountain-front streams in arid and semi-arid parts of the western United States, in particular for channels that form on alluvial fans with coarse, unconsolidated sediment (Niswonger et al., 2005) or in channels on bedrock with high permeability, like carbonates (Scanlon et al., 2006). Channel infiltration is much less important for watersheds on granitic terrain with limited bedrock permeability (Scanlon et al., 2006), though there is currently large uncertainty about the magnitude of channel infiltration for a range of channel properties and geologic settings.

The objective of this document is to compare key flow metrics calculated using 1) observed flow data 2) the SDHM with default parameters, both without and with channel infiltration and 3) the SDHM calibrated for two small, undisturbed watersheds in San Diego County. One of the two watersheds has a small drainage area (0.6 mi^2) and another a larger drainage area (22.4 mi^2). The flow metrics include the flow duration curve (FDC) and flood peaks at different recurrence intervals (Q2, Q5, Q10), calculated from both the annual maximum series and the partial duration series. The report summarizes how the default SDHM parameters differ from the calibrated model, and highlights key differences between the default and calibrated models. The Q2-Q10 values are also compared with regression equations that predict Q2-Q10 from drainage area and mean annual precipitation, including two different regressions from the USGS, one from 1977 (Waananen and Crippen, 1977), a second in 2012 (Gotvald et al., 2012) and a third set of regressions developed specifically for southern California (Hawley and Bledsoe, 2011).

The main questions addressed by the report, as taken from the original scope of work, are:
1. How well do the existing parameterizations of the HSPF model (SD08 and SD11) predict FDCs and peak discharges in small watersheds in San Diego County?

2. What parameters result in a better fit to observed FDCs and peak discharges than the default values?

3. Can parameters of a model calibrated to a large watershed accurately predict peak discharge at a small watershed?

Study sites and data availability

Watersheds were selected that have limited urbanization, small drainage area (<25 mi^2), and available flow data. Two watersheds were selected, Wilson Creek Tributary (USGS Gage 11010900, hereafter "Wilson")(Figure 1) and Guejito Creek (USGS Stream Gage 11027000, hereafter "Guejito").

The Wilson watershed is approximately 23 miles east of downtown San Diego in the Cleveland National Forest. The soil types in Wilson include acid igneous rock in the upper watershed, Las Posas stony fine sandy loam in the central part of the watershed (soil hydrologic group D), and Fallbrook sandy loam in the downstream sections (soil hydrologic group C) (Table 1). Acid igneous rock has rock cover, including large boulders and rock outcrops of acid igneous rock over 50-90% of the surface and no or very shallow soils composed of loamy coarse sand. The Las Posas series is described as "well-drained, moderately deep stony fine sandy loams" but is classified as soil hydrologic group D because of the clay subsoil from 4 to 33 inches deep. The upper 4 inches is stony fine sandy loam, 20-30% stones. The Las Posas series is weathered from basic igneous rock (gabbro). In Wilson, the dominant soil hydrologic group is D (Table 1), which usually has low to moderate infiltration capacities. Vegetation in the Wilson watershed, taken from SANDAG vegetation maps, is "granitic chaparral", "mafic chaparral", and a small area of riparian forest. The most common slope class is very steep (>20 degrees). Steep areas include bedrock outcrops and boulder fields.

The Guejito watershed is approximately 30 miles north-north-east of San Diego and 8 miles east of the City of Escondido (Figure 2). In the Guejito watershed, the soil is mostly in hydrologic groups C and D (Table 1). The dominant soils are sandy loam (16%), rocky sandy loam (15%), stony find sandy loam (10%) and acid igneous rock (6%). More than half (54%) of the soils are classified as stony or rocky. The flat valley bottoms have Fallbrook and Chino sandy loams (Vegetation was mixed forest, chaparral shrub, and grass, with significant bare area on steep slopes and in some sparsely vegetated areas (Figure 3). Land use at Guejito has included ranching (Stallcup et al., 2005). Slopes at Guejito were less steep than at Wilson (Table 1). More detail on the vegetation, soil, and slope categories are in Appendix 1.

The channel bed at Wilson is cobble and sand, with clay channel banks (Appendix 2).

Discharge data: Discharge data were taken from historical records at stream gages maintained by the United States Geological Survey (USGS) (Table 2). Data included daily mean discharge (all stations), 15-minute discharge for limited time periods (Guejito), and the annual peak discharge, which is the annual maximum discharge either the maximum observed at 15-minute intervals (Guejito) or the peak observed instantaneous discharge (Wilson).

The smallest watershed (Wilson) had a relatively short record of daily flows (1967-1973) and a slightly longer record of annual maximum discharge (1962-1973). Initial model calibrations indicated that the hydrologic response to rainfall changed dramatically approximately half-way through the available period of record (1970). Fire perimeter data from SANDAG confirmed that a fire occurred in the watershed in October 1970, coinciding with the observed increase in runoff. Accordingly, the Wilson model was run for only the pre-fire conditions (1961-1970) and calibrated using with both the daily data (1967-1970) and the annual peak discharge observations (1961-1970).

Figure 1. Location map of Wilson Creek Tributary ("Wilson"). Green dots indicate meteorological stations and the purple dot is the USGS stream gage. Insert shows the watershed boundary overlaid on Google Earth imagery.

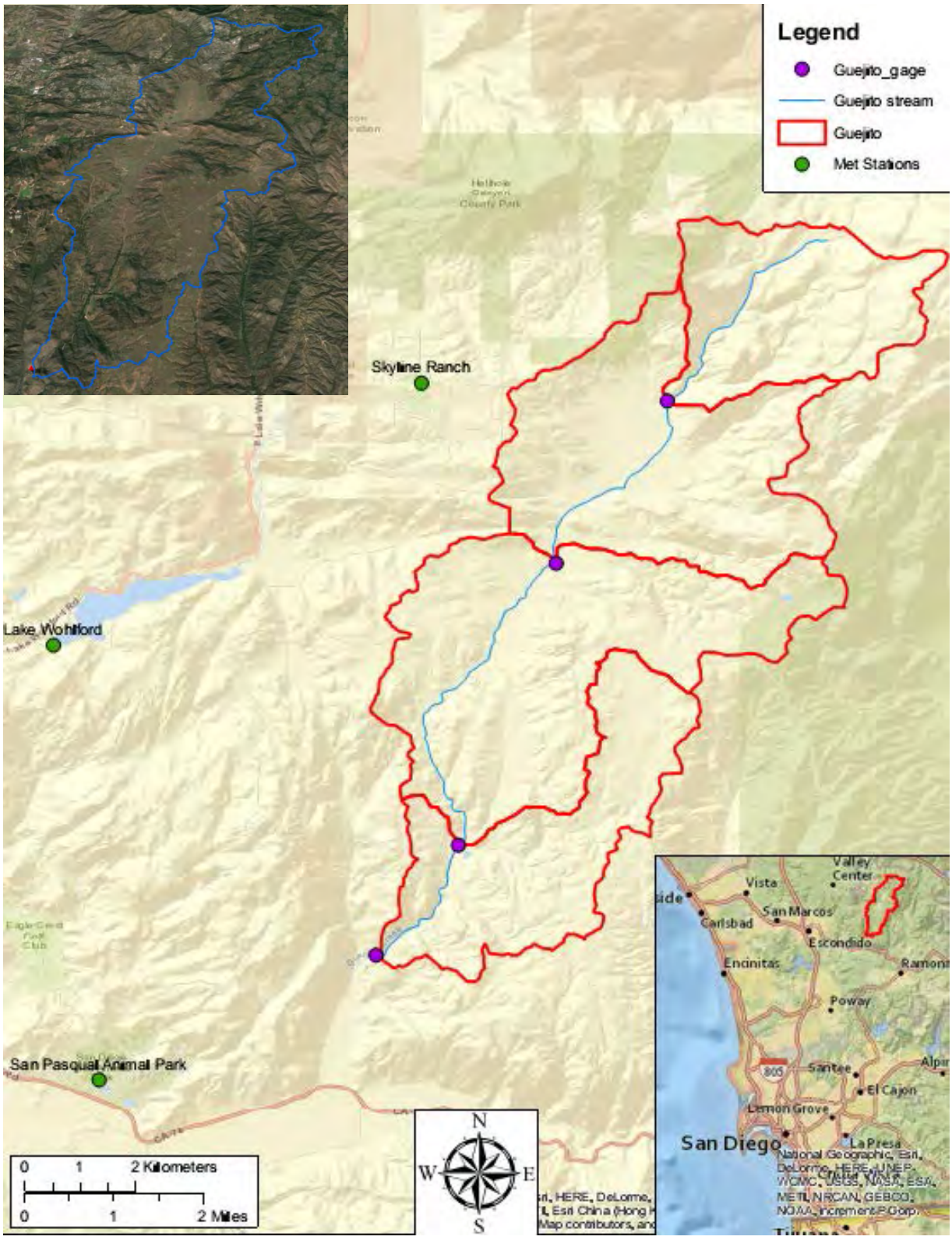

Figure 2. Location map of Guejito Creek ("Guejito"). Green dots indicate meteorological stations and the purple dots indicate the outlets of each of the modelled reaches. Red polygons indicate the sub-watershed boundaries that drain to each modelled reach. The downstream-most outlet is the USGS stream gage.

Table 1. Summary of watershed characteristics. Values for vegetation, soil and slope are % of the watershed area.		
	Wilson	Guejito
Watershed area (mi^2)	0.6	22.4
Vegetation (%)		
Forest	~0	24
Shrub	70	24
Grass	0	24
Bare (rock or soil)	30	29
Soil hydrologic group (%)		
B	0	8
C	9	63
D	91	29
Slope Category (%)		
Flat 0-5	2	17
Mod 5-10	5	18
Steep 10-20	21	29
Very Steep >20	73	36

The Guejito watershed had daily mean and annual peak data for 47 years and 15-minute data for 10 years (2004-2012) (Figure 4). The model for Guejito was calibrated and validated using data from periods without fire (see methods section below). The watershed burned in 2003 and 2007, so much of the 15-minute flow data from that period is likely affected by fire, and the data was not used for calibration or validation of the model.

Rainfall and meteorological data: HSPF requires hourly or better data on rainfall and potential evapotranspiration (PEVT), though daily means can be used for some applications, particularly for prediction of daily or monthly runoff. Meteorological stations were selected based on their proximity to the watersheds and period of record. In some cases, the period of record of PEVT was shorter than that for rainfall. In those cases, the gaps were filled with the mean PEVT calculated for each hour and day using the data from years with data.

Precipitation in HSPF can be scaled by a multiplication factor to reflect differences in precipitation between the meteorological station and the watershed. While the precipitation station nearest Guejito (Skyline Ranch) has insufficient data for the model, it can be compared with the station used for the model (Lake Wohlford) (Table 3). The station data suggests that Lake Wohlford has higher precipitation than the Skyline station for 2005-2007, but long-term mean precipitation from the PRISM model suggests the opposite. Due to lack of alternative data, we used the observed precipitation at Lake Wohlford as input to the model, with a multiplication factor of 1.0.

Table 2. Summary of data available for HSPF modelling at the study watersheds. POR = "period of record." Lake Wolford = CA044726. San Pasqual = CA047874.

Stream Discharge				
Wshed	Station	Mean elev in wshed (ft)	POR (Water Years)	Resolution
Wilson	11010900	2912	1967-1973 1962-1973	Daily Annual peak
Guejito	11027000	2143	1946-1982 1950-1982 2004-2012	Daily Annual peak 15-minute
Precipitation				
Wshed	Station name	Elev.	POR	Resolution
Wilson	Barret Dam CA040514	1621	6/30/1948-12/31/1980	Hourly
Guejito	Lake Wohlford CA 044726	1642	10/08/1949 -12/31/2009 05/03/1971-10/01/1989	Hourly 15-minute
	Skyline	2133	06/30/2004 - 09/29/2013 10/01/2010-09/29/2013	3-Hourly Hourly
ATEM and PEVT				
Wshed	Station name	Elev.	POR	Resolution
Wilson	Barret Dam	1621	6/30/1948-12/31/1980	Hourly
Guejito	San Pasqual CA047874	646	6/30/1979- 10/31/1992	Hourly

Figure 3. Photograph from the summit of Rodriguez Mountain on the northern boundary of the Guejito watershed. Photo credit C. Foster. Note the high soil fraction in the foreground and steep bedrock outcrops.

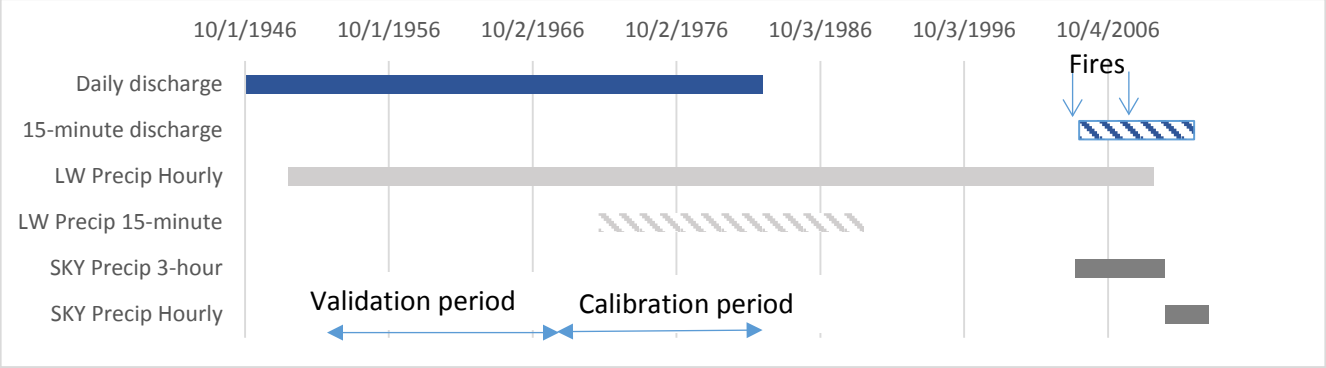

Figure 4. Data overlap diagram for Guejito. LW is Lake Wolhford meteorological station, and SKY is Skyline precipitation station. The model calibration and validation periods have data for both daily discharge and hourly precipitation.

Table 3. Mean annual precipitation at the San Pasqual, Lake Wohlford, and Skyline Ranch raingages where they have overlapping data. Lake Wohlford is the station used for the HSPF model.

	San Pasqual	Lake Wolford CA 044726	Skyline Ranch
2005	28.6	34.5	19.4
2006	5.6	14.6	13.4
2007	5	10.1	7.9
2008	15.3	NA	21.2
2009	11.2	NA	15.4
Mean 2005-2007	13.1	19.7	13.6
PRISM 1981-2010	13.4	16.3	18.6

Methods

The San Diego Hydrology Model (SDHM) is a parameterization of the Hydrological Simulation Program Fortran (HSPF) and was used to develop continuous simulations of discharge at the study watersheds. Two different parameter sets for the SDHM were available:

> SD2011 (SD11): Brown and Caldwell, documented in San Diego Hydrology Manual, January 2012
> http://www.clearcreeksolutions.info/ftp/public/downloads/SDHM/SDHMUserManualJan2012.pdf
>
> SDHM 2008 (SD08): Clear Creek Solutions, documented in San Diego Hydrology Manual, May 2008
> http://www.clearcreeksolutions.info/ftp/public/downloads/SDHM/SDHMUserManualMay2008.pdf

While SD11 is the more recent version of the model and includes wetland processes and parameters, SD08 has more detailed vegetation types (e.g. Forest, Shrubs, Grass, Dirt) compared with SD11 (Grass, Dirt and Gravel) that corresponded more closely with actual vegetation present in the study watersheds. SD11 has identical infiltration parameters compared to SD08, but more loss to deep groundwater (DEEPFR), more loss of water from riparian vegetation and wetlands, and different stormflow recession characteristics.

The period of simulation was determined from the periods of record of discharge data. Due to limited data availability, all available data were used for calibration at Wilson. The record at Guejito was split into calibration and validation periods. The calibration period was chosen to include several large storm events. The modeling time periods were:

Wilson: WY 1962-1970 (10/1/1961-9/30/1970)
Guejito:
Calibration: WY 1966-1981 (10/1/1965-9/30/1981) Mean annual precip = 20.2 in
Validation: WY 1952-1965 (10/1/1951-9/30/1965) Mean annual precip = 14.5 in

Data on annual instantaneous peak discharge were available at Wilson for WY 1962-1970. Daily mean discharge data were only available at Wilson (pre-fire conditions) for WY 1968-1970 (Table 2).

The models were run at 15-minute intervals to correspond with the field data collected on sediment transport during storm events, and to match the USGS methods to calculate peak discharges a various recurrence intervals (Gotvald et al., 2012). Input meteorological data, including precipitation data, were only available at 1 hour resolution, so the model assumed that precipitation was uniform over each 1 hour period. While some 15-minute precipitation data was available for the Guejito watershed (Lake Wohlford), it was not used because 1) the available date range did not overlap with available 15-minute discharge data, 2) the time period of available 15-minute precipitation data was too short (< 20 years) to define flows at large recurrence intervals and 3) the raingage was ~4 miles west of the watershed boundary, so the timing and intensity of precipitation at 15-minute intervals at the gage may differ from the watershed-mean precipitation.

Annual precipitation measured at the raingage used for the model at Guejito (Lake Wohlford) was higher during the calibration period (20.2 inches) than during the validation period (14.5 inches). The calibration period included years with the highest recorded annual total rainfall (Figure 5). The calibrated model therefore includes the full range of peak discharge values that is expected to be observed in the period of record. The Wilson model calibration period includes some wet years, though not the maximum observed over 1951-1992.

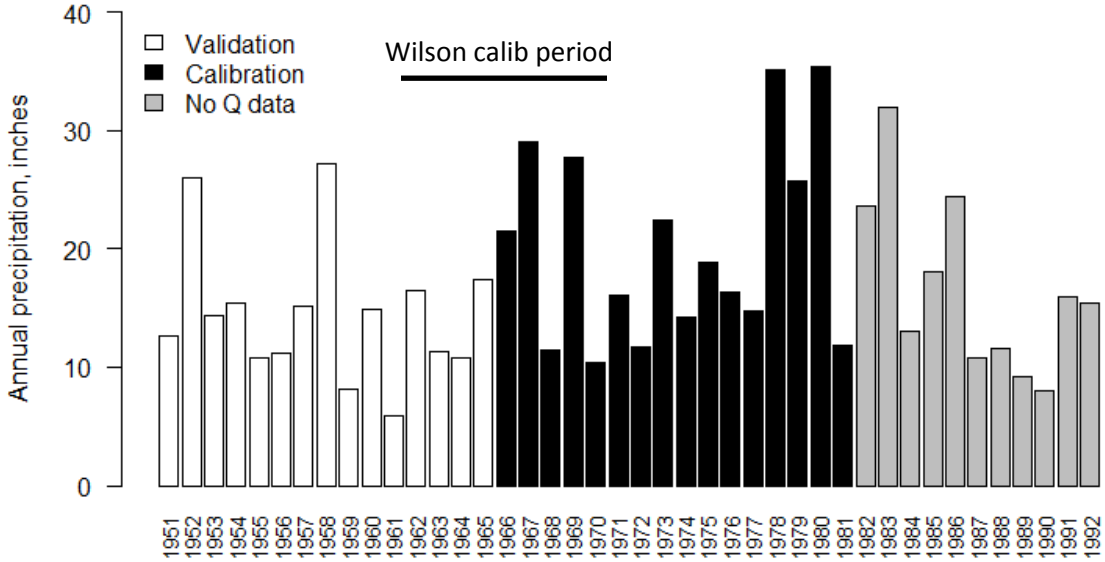

Figure 5. Time series of annual precipitation at the raingage used for the Guejito models (Lake Wohlford). Note that the period includes the highest observed precipitation totals in the 1951-1992 time series.

PERLND categories and areas

The PERLND classes for SD11 include grass, dirt, and gravel. The GIS layer of vegetation did not have a separate category for bare, unvegetated surfaces (called "dirt" in SD08 and SD11), though visual inspection of Google Earth imagery indicated significant cover of soil and bare rock in both watersheds. In order to convert the GIS vegetation categories to categories in the SDHM, a vegetation cover fraction was determined for each vegetation class using visual interpretation of high resolution imagery in Google Earth. Non-vegetated surfaces with no apparent outcropping of rock or conglomerate were assigned "Dirt" cover, while non-vegetated surfaces with outcropping bedrock or cobbles were assigned to "Gravel" cover. In SD11, both default and calibrated versions, infiltration is assumed higher on dirt than on gravel; visual inspection of aerial imagery suggested that much of the gravel category was actually mostly exposed bedrock and boulder fields (Figure 3), which are assumed to have lower point-scale infiltration rates than dirt. Runoff generation from gravel is not significantly different from the dirt category because upper zone soil moisture is higher in gravel, which slows overland flow and increases total infiltration rates. The final areas of each pervious land unit (PERLND) are listed in Appendix 1.

PEVT parameters

There was a large difference between annual total potential ET (PEVT) reported in the EPA BASINS database and annual total reference ET from the California Irrigation Management Information System (CIMIS), which is regarded as the most reliable dataset for PEVT. PEVT in BASINS is calculated with the Hammon formula for reference ET, which may not be applicable to coastal regionals like

California. Reference ET from CIMIS is calculated using the Penman equation and is the accepted standard for California (Bekele et al., 2005). Neither SDHM report (SD08 or SD11) provides values for the multiplier for PEVT, which converts the observed values of PEVT reported at the meteorological station to values that approximate lake evaporation or reference ET. For the Wilson and Guejito models, the PEVT multiplier was calculated as the ratio between mean annual reference ET from the CIMIS dataset and the mean annual PEVT from the meteorological stations. There was a large difference between PEVT in BASINS at Wilson (31.6 inches) and reference ET from CIMIS (55 inches), requiring the use of a PEVT multiplier in the SDHM of 1.74 (55 inches/31.6 inches). For Guejito, the PEVT parameter was set to 1.60 to realize annual PEVT of 55 inches. Here PEVT and reference ET are considered equivalent, since both Penman and Hammon formulas are described in the literature as methods to estimate reference ET (Bekele et al., 2005; Lu et al., 2005)

Channel routing and reach geometry

HSPF uses storage-based routing in channels, where the volumetric change in a reach is proportional to the weighted sum of the inflow to and outflow from the reach. The user specifies the relationship between depth, planimetric water area, volume, and discharge for each reach, and the weighting coefficient (KS) which is assumed to be 0.5, corresponding to wave translation without attenuation. For the Wilson and Guejito models, the depth-discharge relationships were taken from USGS rating curves. For Guejito, USGS data was available on width and depth of flow. For Wilson, width and depth were determined from field surveys (Appendix 2). HSPF allows for the channels in the watershed to be divided into reaches. For Wilson, a single reach was used. For Guejito, four reaches were used based on the watershed area and tributary junctions (Figure 2). RCHRES 46 was designated as the downstream-most reach, and reaches 43, 44, and 45 were upstream reaches.

Reach geometry and the corresponding data required for the FTABLES, including planimetric area of water, volume of water, and discharge at the downstream point, all as a function of water depth, were taken from USGS gaging station data and channel cross sections collected in July, 2014 (Wilson) (Appendix 2). Wilson had data on gage height and stream discharge, but no data on channel geometry. Accordingly, three channel cross sections were collected at three locations in Wilson in July, 2014. Reach geometry at the downstream-most reach of Guejito (RCHRES 46) were taken from channel surveys from the USGS at the downstream site. The reach geometry for the other three reaches were calculated as the product of the value at RCHRES 46 and the drainage area to the outlet of the reach divided by the drainage area at the outlet of RCHRES 46. Discharge at each of the three upstream reaches was calculated using the Manning equation, where slope was taken as the reach-average slope.

Model calibration

SD08 and SD11 were initially run with the default parameters. Calibration was then performed, using the HSPEXP+ expert system and physical interpretation as a guide (e.g. infiltration and soil moisture stores should be lower on higher slopes due to higher rock cover, and higher for vegetation). First, the annual water balance was matched to within 10% of the sum over the study period. Next, the flow duration curves of daily mean discharge were matched, both visually and using statistics of the highest 1% and 5% of mean daily flows. Finally, the model predictions of annual peak discharge at 15-minute intervals were compared with the annual peak discharge observed at the USGS gage. At Wilson, the annual water balance and daily-mean FDC comparisons were based on WY 1968-1970. Peak discharge based on 15-minute data were available for WY 1962-1970. No daily data was available

from 1962-1967 at Wilson, but annual maximum flow (15-minute interval) was available from WY 1962-1970.

The calibration process included some implicit assumptions about the hydrologic properties of the three cover types (vegetation, gravel, dirt). In the original SD11, gravel has a lower infiltration rate but high upper zone soil moisture storage (UZSN) than dirt or grass, presumably because of detention storage among surface fragments. By contrast, many laboratory experiments and field work, often on agricultural soils, suggest that surficial rock fragments decrease overland flow velocities and prevent surface sealing by rain drops, which together increase infiltration rates (Cerdà, 2001; Grant and Struchtemeyer, 1959). This is the opposite of the assumption in SD11, where gravel produces more runoff than bare soil. However, the impact of rocks on infiltration rates depends on the position of the rock in the soil profile: rocks on the surface increase infiltration rates by retarding overland flow velocities, but rocks embedded in the soil reduce infiltration rates (Poesen et al., 1990), and overall rocks in the soil profile reduce hydraulic conductivity and reduce infiltration rates (Brakensiek and Rawls, 1994). For boulder-mantled soils and rock outcrops on steep slopes, which accounts for much of the rocky soil types in Wilson and Guejito, runoff generated on rocks that runs off to adjacent soil may exceed the infiltration rate of receiving soil, resulting in a positive relationship between rock cover and runoff generation (Yair and Lavee, 1976). In shrub-dominated landscapes in semi-arid climates, stone cover correlates with decreased infiltration rates, because sandy soils with high infiltration rates accumulate under shrubs, while between vegetation sands and organic matter were eroded by rainfall, resulting in surface sealing and stone pavement that has low infiltration rates (Abrahams and Parsons, 1991; Wilcox et al., 1988). Together, the field data suggest that infiltration rates decrease with increasing rock cover under natural conditions where rocks are both on the surface and embedded in the soil profile, and under rock outcrops and boulders. For this reason, we maintained the higher INFILT values on gravel.

INFILT parameters in HSPF are recommended to range between 0.01 and 0.25, and interflow (INTFW) between 1 and 3. A suggested formula to relate INFILT and INTFW to measurable infiltration rates is I = 2*INFILT*INTFW. The HSPF guidebook lists the following as reasonable values for I:

SCS Hydrologic Soil Group	INFILT Estimate (in/hr)	(mm/hr)	Runoff Potential
A	0.4 - 1.0	10.0 - 25.0	Low
B	0.1 - 0.4	2.5 - 10.0	Moderate
C	0.05 - 0.1	1.25 - 2.5	Moderate to High
D	0.01 - 0.05	0.25 - 1.25	High

Infiltration experiments on natural landscapes in semi-arid environments report steady-state infiltration rates measured with a small-footprint infiltrometer of between 120 mm/hr to >260 mm/hr on pine forest and mixed conifer landscapes (Martin and Moody, 2001) (soil type not reported, developed on "igneous rock"). Vegetation has profound impacts on infiltration; for one site in arid Australia, infiltration under vegetation, measured with single-ring disk infiltrometers, was 3-5 times that of inter-canopy areas (Dunkerley, 2000), where infiltration was 30 mm/hr under vegetation and 3-4 mm/h on bare soil, though the disk technique underestimates infiltration rates on soils with roots and macropores. In many chaparral landscapes, infiltration capacities are high enough to prevent overland

flow for most rainfall events. In a chaparral landscape of southern California on type D soils (silty clay loams with smectitic-type clays), infiltration rates were > 140 mm/hr measured by a sprinkling infiltrometer (Fierer and Gabet, 2002). If INTFW is kept at 2, then 140 mm/hr (5.5 in/hr) corresponds to INFILT of 2.8, which is higher than the 0.25 recommended.

Parameters for the model calibrated to the large watershed (Guejito) were applied to the small watershed to test for the transferability of parameters. While it would be useful to also transfer parameters from the small watershed to the large, the small watershed was dominated by D-type soils, while the large watershed had a significant fraction of C-type soils. The lack of C-type soils in the small watershed means that the parameter values are not well constrained for C-type soils. While the parameters for the C-type soils could be taken from the calibrated model at the large watershed and the parameters for the D-type soils from the small watershed, this mix would prevent a good test of transferability of parameters from small to large watersheds.

Channel infiltration was not initially included in any of the HSPF models. In order to estimate the potential impact of channel infiltration on model results, a channel loss component was added to the FTABLE in the Wilson model. The channel loss magnitude in a given reach (cfs) was calculated as:

$$F = fA$$

where f is a constant channel infiltration rate used in previous models of channel infiltration in Baja California (6.2 in/hr) (Ponce et al., 1999) and A is the planimetric area of wet channel as provided in the FTABLE (Appendix 2). This method follows others who have used HSPF to simulate the impact of channel infiltration in watersheds in southern California (Guay, 2002). The value used by Ponce et al. (1999) corresponds to channels on unconsolidated alluvium with high infiltration rates. Other, lower values of channel infiltration have been reported for other watersheds in the western United States, in particular 2 in/hr in Western Nevada in a channel bed of cobble and sand (Table 4), though the rate from Western Nevada is for saturated conditions, and infiltration rates under unsaturated conditions were higher (4-6 in/hr) (Figures 6 and 10 in Ronan et al, 1998). At Wilson, the channel bed is a mixture of cobble and coarse sand (Appendix 2) but the sediment is underlain by bedrock, so high infiltration rates are likely at the surface but the true rate is unknown. In order to simulate the maximum likely impact of channel infiltration on model results, we used the higher value (6.2 in/hr) (Ponce et al., 1999), recognizing that this may be an overestimate. The goal of including channel infiltration is not to accurately account for actual channel infiltration losses, but rather to illustrate its potential importance for model calibration and predictions.

Table 4. Literature values of channel infiltration rates.

Geographic location or material type	Channel infiltration (in/hr)	Source
Baja California[a]	6.2	Ponce et al, 1999
Gravel, coarse sand	>5	Land, 1984
Clean sand and gravel	2-5	Land, 1984
Western Nevada	2	Ronan et al, 1998
Sand and gravel with low silt and clay content	1-3	Land, 1984
Sand and gravel with high silt and clay content	0.25-1.0	Land, 1984

a. Taken from Matlock (1965).

Observations and predictions of Q2-Q10

Q2, Q5 and Q10 (hereafter Qx) were determined for the period with observed peak discharge data using both the annual maximum series (15-minute peak) and the partial duration series (daily mean flow). The partial duration series allows for multiple large events in a single year, but it must be remembered that the daily mean will miss short-duration peaks that are important in small watersheds.

For the annual maximum series, the Weibull plotting positions and recurrence intervals (Tr) were calculated for each flow, and Q2-Q10 determined from the rank-ordered annual peak flows. Predictions of Qx were made for the original SD08 and SD11 without calibration, SD11 with channel infiltration, calibrated SD11 at Wilson (without channel infiltration), calibrated SD11 at Guejito (without channel infiltration), and USGS regression equations (Table 5).

Q2, Q5 and Q10 (Qx) from the partial duration series were calculated for mean daily flow, because 15-minute flow values were only available for the annual maxima. Qx from partial duration depend on 1) a flow threshold and a gap in days (GAP), which together define storms. A storm is defined as the period of time over which the discharge is above the flow threshold continuously with a maximum gap of GAP days. The storm peak is the maximum daily discharge observed over that storm period. Here we used a flow threshold of 0.002 cfs/acre and a gap of 1 day.

Regressions from the USGS and Hawley and Bledsoe (2011) were also used to calculate Qx (Table 5). Original USGS regressions are from Waananen and Crippen (1977), hereafter USGS1977. A revision to the USGS regressions were presented in Gotvald et al. (2012), hereafter USGS2012. A third set of regressions was developed by Hawley and Bledsoe (2011) hereafter H&B2011. The regression equations predict maximum annual discharge observed in 15-minute intervals. The equations used from USGS2012 were for the South Coast (Region 5), in Table 5 of Gotvald et al (2012) (Table 5). The H&B2011 regressions included a parameter for impervious cover (I%), which was 0 for both Wilson and Guejito.

Table 5. USGS regression equations used to predict Q2-Q10 from drainage area and mean annual precipitation, South Coast (Region 5) (Table 5 in Gotvald et al., 2012). Q is based on the annual maximum series observed in 15-minute intervals.

Model name	USGS2012	USGS1977	H&B 2011
Reference	(Gotvald et al., 2012)	(Waananen and Crippen, 1977)	(Hawley and Bledsoe, 2011)
Q2	$3.60(A^{0.672})(P^{0.753})$	$0.14(A^{0.72})(P^{1.62})$	$0.53(A^{0.667})(P^{1.29})(e^{8.61*I\%/100})$
Q5	$7.43(A^{0.739})(P^{0.872})$	$0.40(A^{0.77})(P^{1.69})$	$8.5(A^{0.838})(P^{0.773})(e^{3.23*I\%/100})$
Q10	$6.56(A^{0.783})(P^{1.07})$	$0.63(A^{0.79})(P^{1.75})$	$18.2(A^{0.868})(P^{0.767})(e^{0})$

Comment on flow durations for use with geomorphologic calculations

Geomorphologists prefer to use the partial duration series defined using discharge data with short intervals (e.g. 15-min) to estimate Qx, because the partial duration series represents the frequency of high flows, regardless of whether they occur in the same year, and short intervals are more relevant than daily averages for sediment transport processes. Here, the annual maximum series is also used to evaluate the SDHM models because 1) there were insufficient data to quantify Qx for the short intervals (15-minutes) relevant for geomorphological processes; Qx from the partial duration could only be calculated for daily mean discharge and 2) other methods, including the regression equations in Table 5, are based on the annual maximum series. Good model predictions of Qx from the daily mean

partial duration series do not necessarily imply good predictions of 15-minute Qx, so the comparison of model results using partial duration series must be made cautiously.

Results

1. How well does the existing parameterization of the HSPF model (SD08 and SD11) predict FDCs and peak discharges in small watersheds in San Diego County?

Annual discharge and flow duration curves

The SD08 model over-predicted the annual water balance, discharge at all flow exceedence percentages and peak discharges compared to the observed data for both Wilson and Guejito watersheds (Tables 5-9, Figure 6, Figure 7, Figure 8, Figure 9). SD11, by contrast, had acceptable errors in the annual water balance (-12%) and in Q1% and Q5% at Guejito, with larger errors at Wilson (Table 6, Table 8). SD11 slightly overpredicted high flow but underpredicted low flow significantly at Guejito; the opposite was observed at Wilson. The calibrated models fit the observed flow duration curves well in both watersheds, with small errors in the annual water balance and good matches with the observed flow duration curves (Figure 7, Figure 9).

Inclusion of channel infiltration improves the annual water balance and flow duration curve for SD11 at Wilson, but did not significantly reduce errors in Qx (Table 7). The calibrated model with channel infiltration had the best fit to the flow duration curve at Wilson (Figure 7), but had higher error in predicting Qx than the calibrated SD11 without channel infiltration (Table 7). Inclusion of channel infiltration in the SD11 model of Guejito resulted in unrealistically low baseflow (Figure 9). Due to the large watershed size and underlying igneous geology, channel infiltration upstream may return as baseflow downstream and may not be an important process at Guejito.

Peak discharges (Q2, Q5, Q10). SD08 overpredicted peak discharges at both Wilson and Guejito, with the largest overprediction of up to 17 times for annual maximum Q2 at Wilson (Table 7, Table *9*, Figure 12, Figure 13). SD11 performs significantly better than SD08 but still has high errors in Q2 at Wilson (12 times observed). The calibrated SD11 model performed very well at Wilson, with errors of 25% (Q2) and 5% or less for Q5 and Q10. The Wilson model with channel infiltration had high errors in peak Q, despite the good agreement with the daily flow duration curve. At Guejito, SD11 had a good fit to peak Q, with model errors of less than 140% for the annual maximum series and less than 60% for the partial duration series. The calibrated SD11 at Guejito had lower error in both calibration and validation periods, except Q5 and Q10 for the partial duration series in the validation period (Figure 16, Table 10). The USGS2012 equations performed surprisingly well, with roughly similar error in predictions of Q5 and Q10 compared with the calibrated model, though USGS2012 overpredicted Q2 by ~4 times at Wilson and by 2 times at Guejito. USGS1977 predicted Q2 more accurately than USGS2012, but underpredicted Q5 and Q10. The regression model of Hawley and Bledsoe (2011) performed very well at Wilson but overpredicted Q5 and Q10 at Guejito.

The error in model predictions of Qx decreased with the duration for the partial duration series, but not for the annual maximum series (Figure 15).

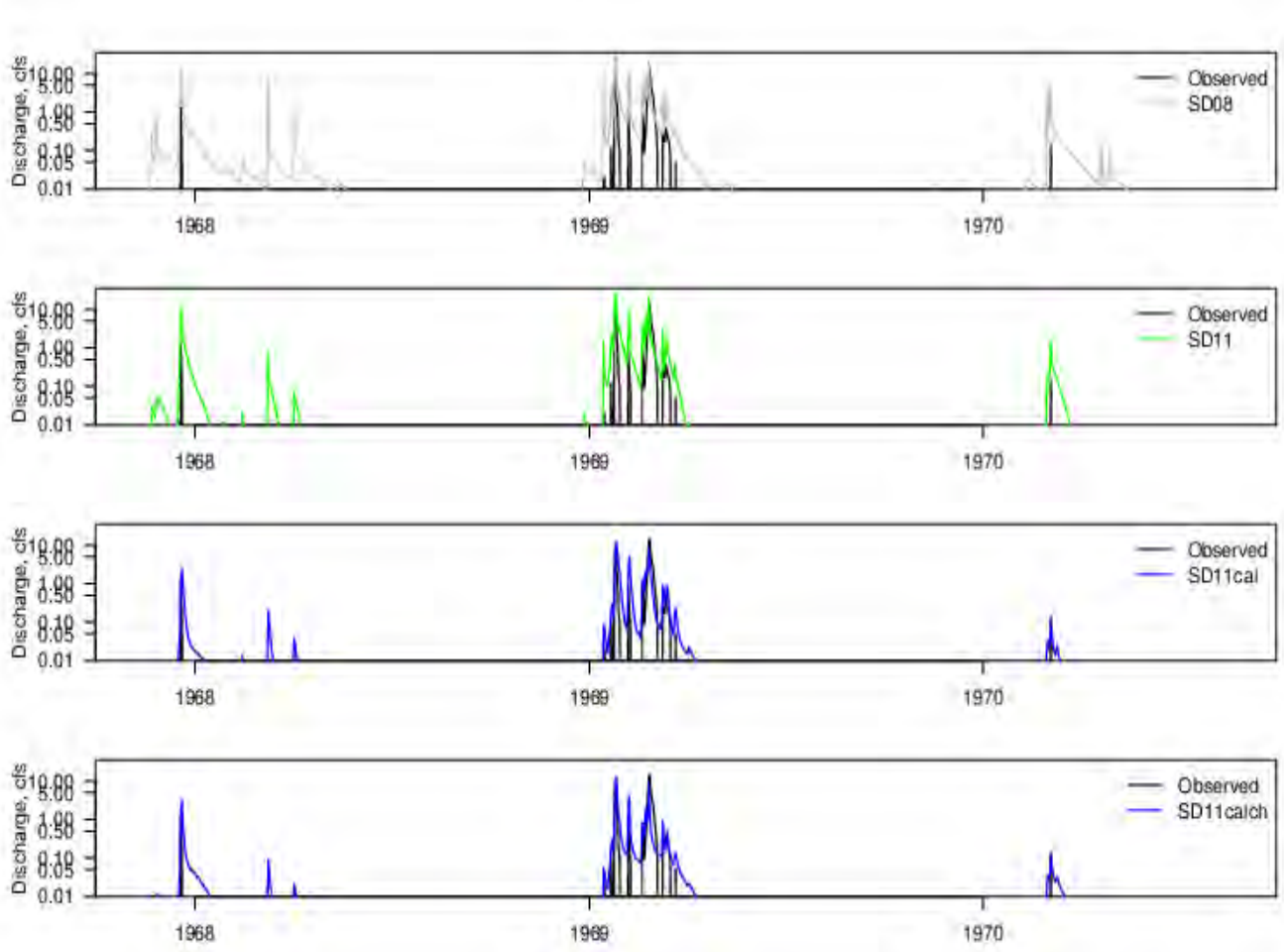

Figure 6. Time series of observed and simulated daily discharge at Wilson, SD08, SD11, and calibrated SD11 model without channel infiltration (SD11cal) and with channel infiltration (SD11calch).

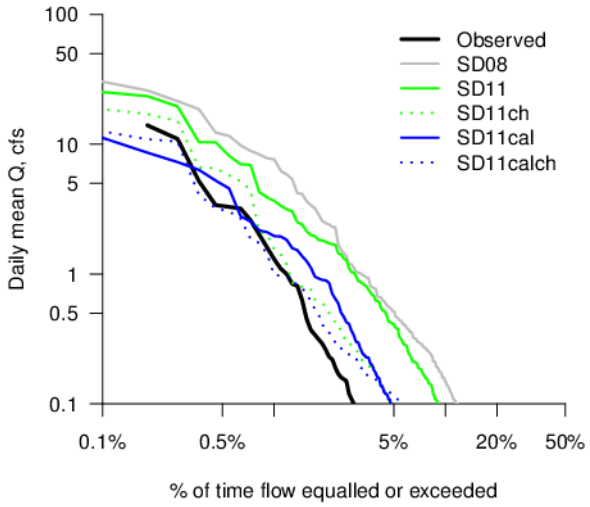

Figure 7. Flow duration curves for five models at Wilson, including the default SD08, default SD11 without channel infiltration (SD11) and with channel infiltration (SD11 ch), and the calibrated SD11 model without channel infiltration (SD11cal) and SD11 with channel infiltration (SD11calch). Modelled period covers 1967/10/01 to 1970/09/30.

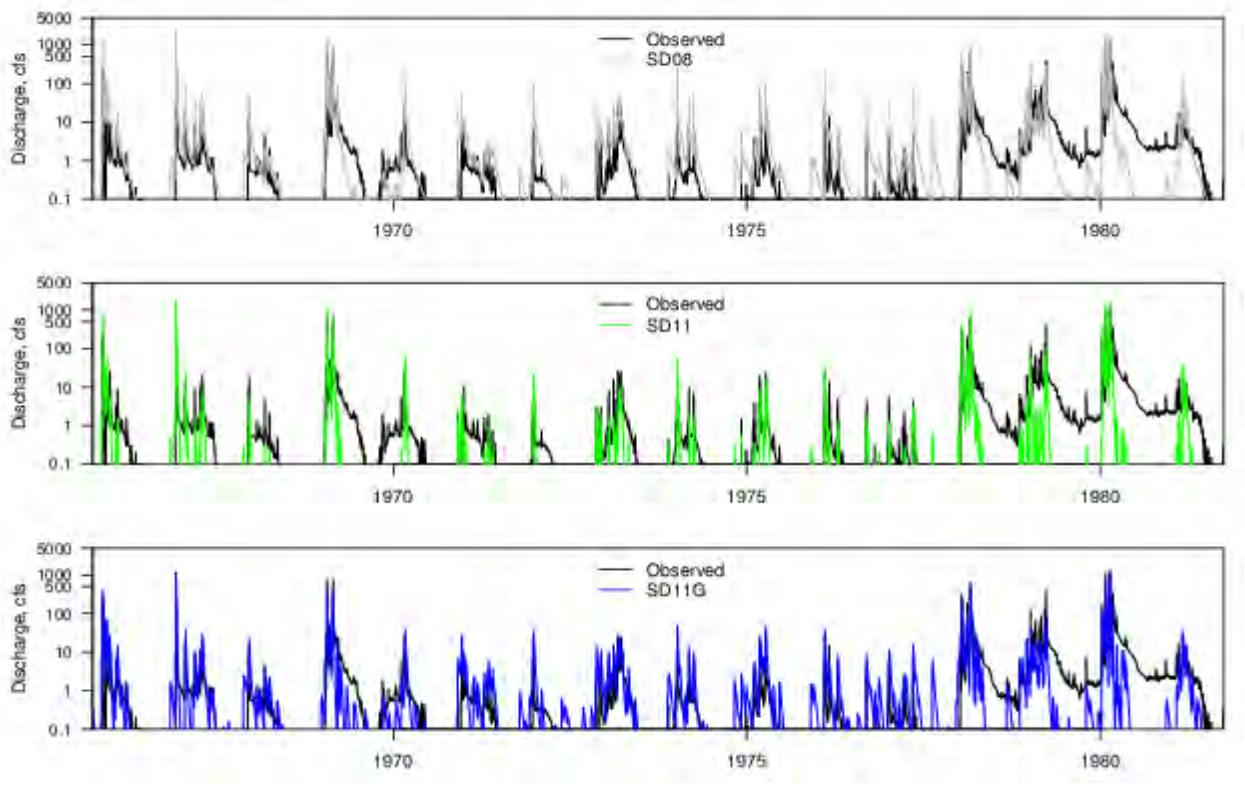

Figure 8. Time series of observed and simulated daily discharge for Guejito during the calibration period for SD08 (top), SD11, and calibrated SD11.

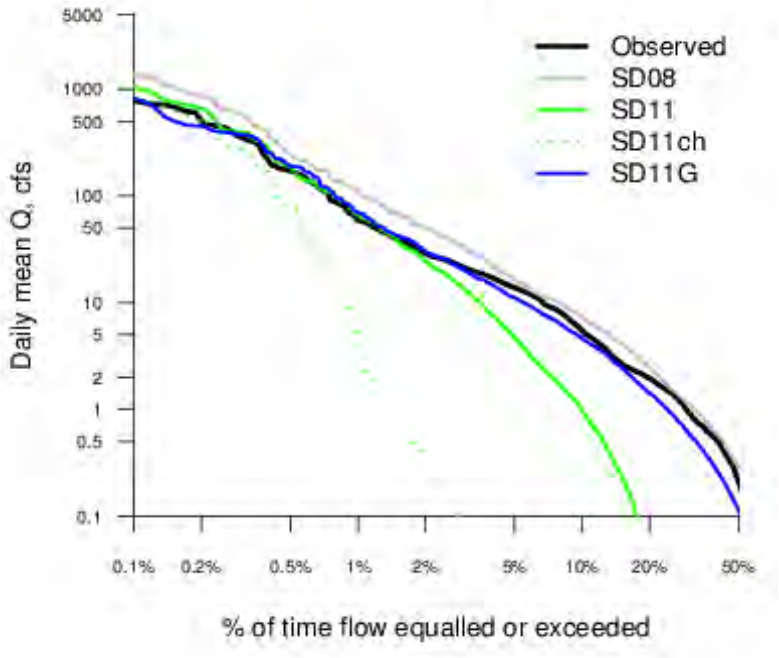

Figure 9. Flow duration curves of mean daily discharge for Guejito during the calibration period, including observed, SD08, SD11, SD11 with channel infiltration (SD11ch), and calibrated SD11 without channel infiltration (SD11cal).

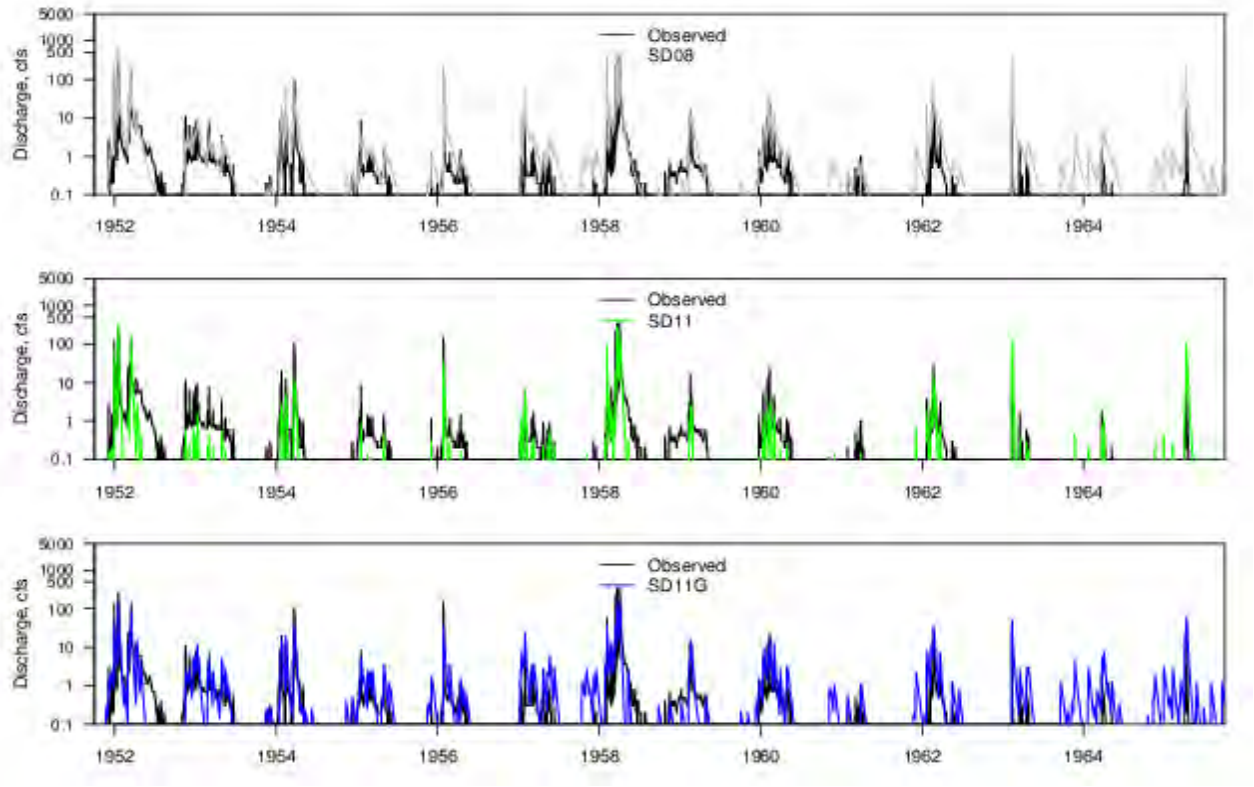

Figure 10. Time series of observed and simulated daily discharge for Guejito during the validation period for SD08, SD11, and calibrated SD11.

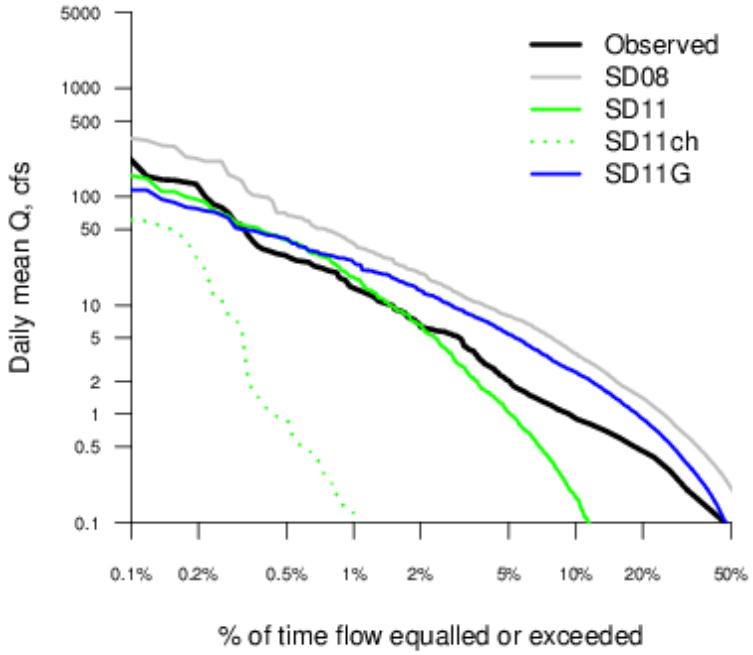

Figure 11. Flow duration curves of mean daily discharge for Guejito during the validation period, including observed, SD08, SD11, SD11 with channel infiltration, and calibrated SD11 without channel infiltration.

Table 6. Summary statistics of annual and low percentage flows at Wilson, including observed and modelled discharge. Q percentiles are from 3 years of daily data. Q1% and Q5% are the mean of all daily discharge values that are greater than the 1% and 5% exceedence defined from the flow duration curve.

	Annual		Q1%		Q5%	
	Q	**% error**	**Q**	**% error**	**Q**	**% error**
Observed	0.06	-	7.1	-	1.7	-
SD08	0.25	317	15.6	120	4.5	165
SD11	0.17	183	12	69	3.3	94
SD11ch	0.1	67	8.4	18	1.9	12
SD11W	0.07	17	5.1	-28	1.4	-18
SD11Wch	0.06	0	5.2	-27	1.2	-29
SD11G	0.15	150	7.6	7	2.7	59

Table 7. Q2-Q10 at Wilson for the annual maximum series, including observed and modelled estimates. Qx are from 10 years of the annual 15-minute maximum.

	Q2		Q5		Q10	
	Q	**% error**	**Q**	**% error**	**Q**	**% error**
Observed	4	-	62	-	98	-
SD08	74	1750	235	279	249	154
SD11	52	1200	185	198	219	123
SD11ch	42	950	171	176	201	105
SD11W	6	50	64	3	97	-1
SD11Wch	6	50	86	39	166	69
SD11G	14	250	75	21	112	14
USGS2012	20	400	54	-13	80	-18
USGS1977	8	100	26	-58	48	-51
H&B 2011	12	200	45	-27	93	-5

Table 8. Summary statistics of annual and low percentage flows at Guejito, including observed and modelled discharge for the calibration and validation periods. All Q values are in cfs. Q percentiles are from daily data. Q1% and Q5% are the mean of all daily discharge values that are greater than the 1% and 5% exceedence defined from the flow duration curve.

	Annual		Q1%		Q5%	
	Q	**% error**	**Q**	**% error**	**Q**	**% error**
Calibration period						
Observed	5.1	-	313	-	83	-
SD08	7.8	53	496	58	130	57
SD11	4.5	-12	364	16	87	5
SD11G	4.8	-6	300	-4	80	-4
Validation period						
Observed	1.1	-	70	-	18	-
SD08	2.7	145	135	93	39	117
SD11	0.9	-18	64	-9	17	-6
SD11G	1.4	27	53	-24	19	6

Table 9. Q2-Q10 at Guejito for the annual maximum series, including observed and modelled estimates for the calibration and validation periods. Qx are from the annual 15-minute maximum.

	Q2		Q5		Q10	
	Q	**% error**	**Q**	**% error**	**Q**	**% error**
Calibration period						
Observed	89	-	2183	-	3132	-
SD08	1020	1046	5792	165	6625	112
SD11	132	48	5279	142	6373	103
SD11G	51	-43	1619	-26	3179	2
USGS2012	280	215	1019	-53	1871	-40
USGS1977	171	92	706	-68	1417	-55
H&B 2011	202	127	1175	-46	2717	-13
Validation period						
Observed	71	-	457	-	1194	-
SD08	285	301	1987	335	3815	220
SD11	7	-90	786	72	1969	65
SD11G	30	-58	124	-73	293	-75
USGS2012	220	210	770	68	1327	11
USGS1977	102	44	410	-10	808	-32
H&B 2011	134	89	917	101	2124	78

Table 10. Q2-Q10 at Guejito for the partial duration series of daily mean discharge (cfs), including observed and modelled estimates for the calibration and validation periods.

	Q2PD		Q5PD		Q10PD	
	Q	**% error**	**Q**	**% error**	**Q**	**% error**
Calibration period						
Observed	249	-	852	-	1173	-
SD08	665	167	1403	65	1783	52
SD11	394	58	1087	28	1420	21
SD11G	190	-24	573	-33	998	-15
Validation period						
Observed	131	-	260	-	345	-
SD08	233	78	403	55	514	49
SD11	70	-47	201	-23	297	-14
SD11G	42	-68	125	-52	137	-60

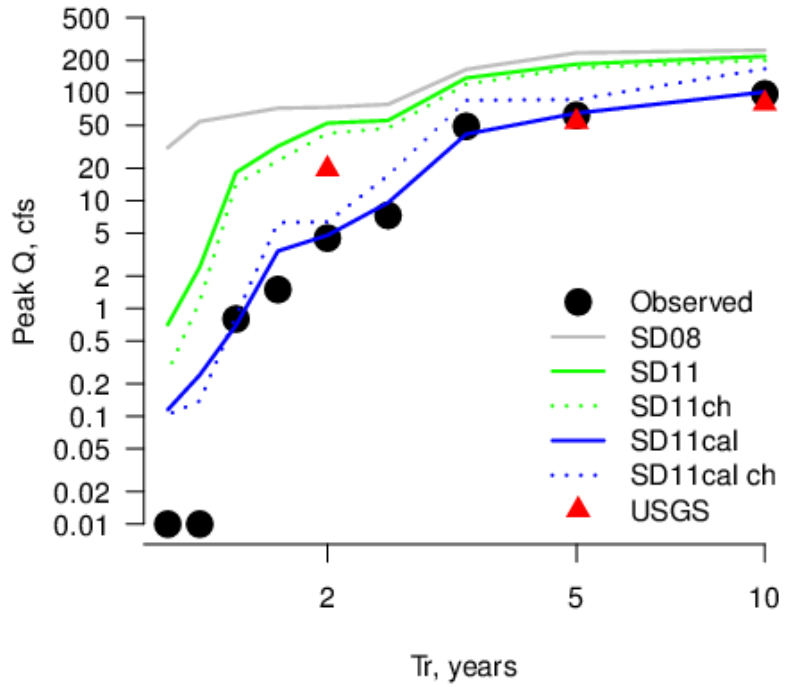

Figure 12. Annual peak Q versus recurrence interval for Wilson. USGS regression is from USGS2011.

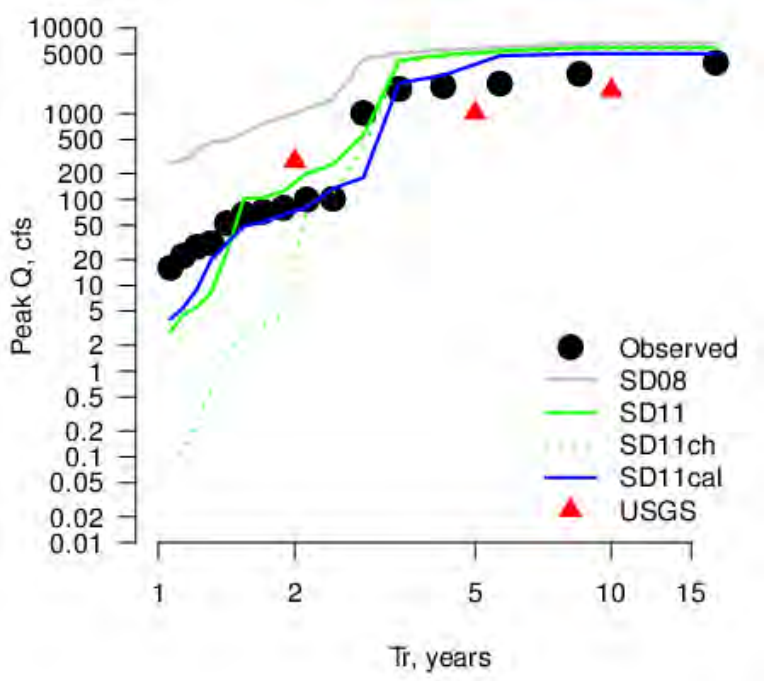

Figure 13. Annual peak Q versus recurrence interval for Guejito during the calibration period. USGS regression is from USGS2011.

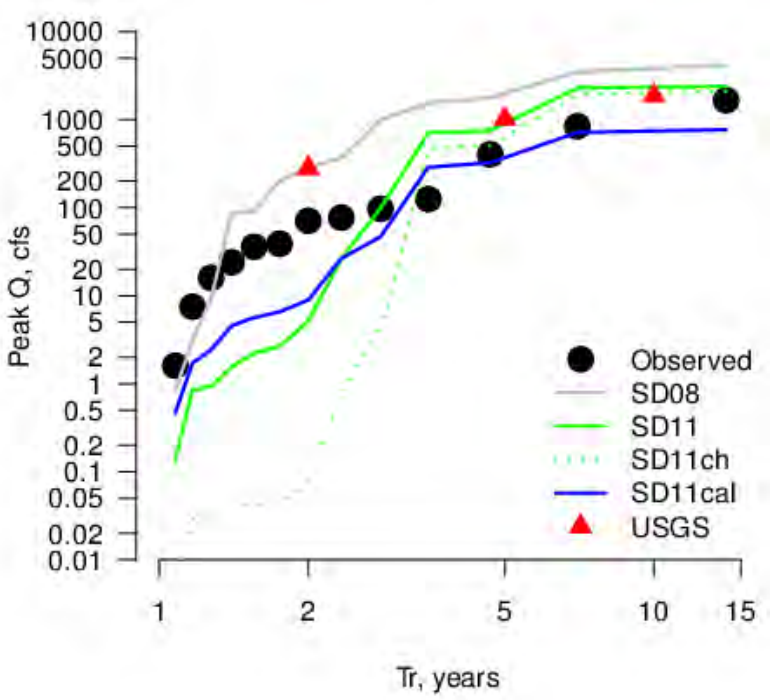

Figure 14. Annual peak Q versus recurrence interval for Guejito during the validation period. USGS regression is from USGS2011.

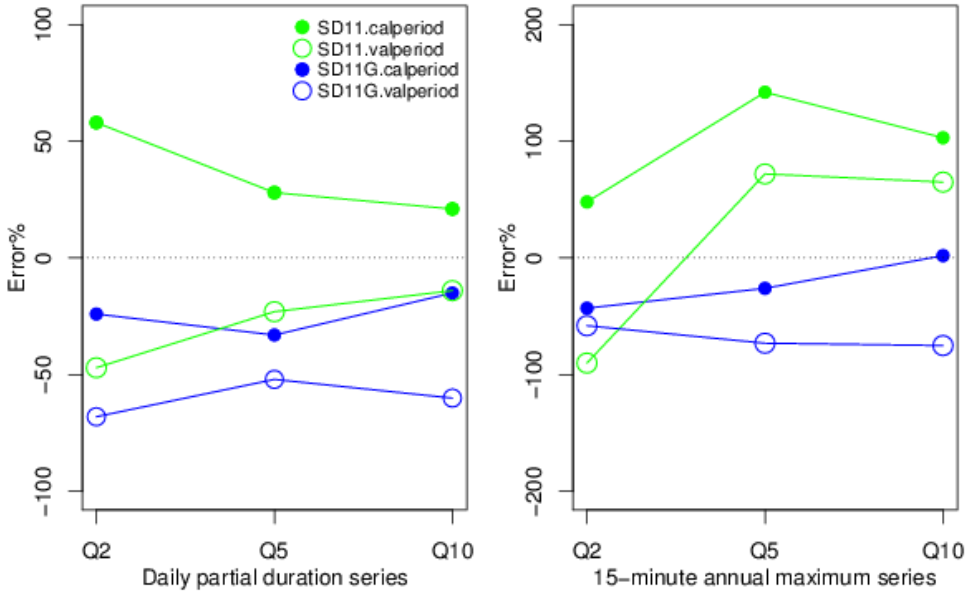

Figure 15. Error in peak discharge estimation versus the return interval at Guejito, during both calibration period and validation period.

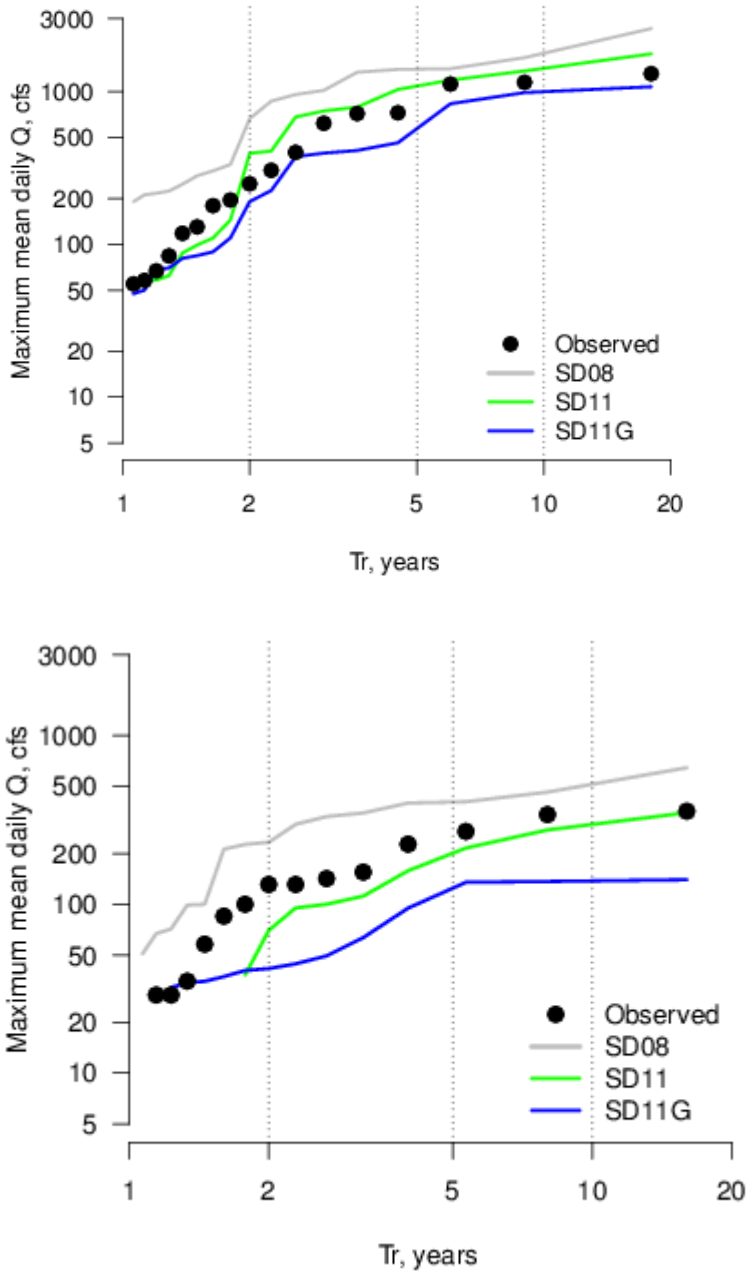

Figure 16. Maximum mean daily flow for Guejito for the calibration period (top) and validation period (bottom), calculated using partial duration series, a flow threshold of 5.6 cfs, and a gap of 1 day on either side of the event.

2. What parameters result in a better fit to observed FDCs and peak discharges than the default values?

Parameter comparison and interpretation

SD11 overpredicted peaks, in particular at Wilson, but underpredicted low flows at Guejito. For the SD11 calibration, the most important changes to the parameters were increases in INFILT, increased soil moisture storage capacity in both upper (UZSN) and lower (LZSN) soil zones (LZSN was adjusted for Wilson model only), and increased interflow parameter INTFW (Table 11, Table 12, Table 13).

INTFW was 0 in SD11 for gravel cover, which may be unrealistic given that UZSN is very high for gravel in SD11. The calibrated model has increased values of UZSN on grass, which was lower than UZSN for bare dirt in SD11.

The increase in INFILT is consistent with other reviews of the SDHM, which have also concluded that SD11 has low INFILT values compared with two other HSPF models implemented for watersheds in San Diego County, particularly for soil types A and B (Tetra Tech, 2011).

The parameter that allows for loss from groundwater to outside the watershed boundary (DEEPFR) was significantly higher than recommended by the US EPA for SD11W (DEEPFR=0.9) (Table *12*) (United States Environmental Protection Agency, 2000), but the high value was responsible for reducing baseflow and storage in the lower soil zone, and good fits to the observed streamflow were not possible without large values of DEEPFR. High DEEPFR may reflect the importance of channel infiltration or other losses through fractured bedrock at Wilson. The parameter describing the amount of ET derived from baseflow (BASETP) was also at the high-end of the recommended range in SD11W, suggesting that the calibrated model without channel infiltration must assume very large unaccounted for losses to deep groundwater, high riparian ET, and high soil moisture storage in order to reproduce the observed annual and daily discharge. SD11G had a lower DEEPFR (0.2) than the default value (0.4), possibly due to Guejito's larger watershed area, where any water that infiltrated into the channel or deep groundwater may re-emerge as baseflow later in the storm or year rather than leave the watershed through subsurface flow.

The partitioning of precipitation into baseflow, interflow, and surface runoff differed by model, and point to some deficiencies in the SD11 model. As an example, runoff from steep slopes with C and D type soils can be compared for the default SD11 and calibrated SD11 (Table 14). Contrary to expectation and field experience in many regions, runoff was greater from grass than from dirt and gravel, with gravel producing the lowest total and lowest storm runoff. This is due in part to the fact that interception and lower zone ET parameters (LZETP) were the same for vegetation and bare surfaces. Grass also had very high interflow values and low upper zone soil moisture storage in the default SD11. By contrast, the calibrated SD11 models have more runoff from gravel and dirt than from grass, which is more consistent with field observations. Grass and dirt have similar runoff production on C-type soils because many parameters were kept constant, since bare dirt did not occur in single homogeneous areas but rather was interspersed throughout the vegetation in a mix mosaic (Figure 3). Thus, the infiltration rate was assumed to be higher on grass than on dirt, but dirt had the same lower and upper zone soil moisture storage as grass.

3. Does incorporation of channel infiltration into the model structure improve model performance or plausibility and interpretation of model parameters?

Incorporation of channel infiltration improved the fit of the SD11 to observed annual and daily mean discharge at Wilson (SD11Wch in Table 6 and Table 7), but did not significantly affect the estimates of peak discharge, perhaps because channel infiltration is a small fraction of discharge at peak discharges. Incorporation of channel infiltration in the calibrated model at Wilson did not significantly improve model errors. The calibrated model with channel infiltration under-predicted the highest daily flows but over predicted peak discharges, suggesting that channel infiltration was overestimated at low flows, and that other changes in model parameters, such as lower infiltration capacity and lower soil moisture storage, generated excessive runoff during peak events. Like the SD08, channel infiltration in the calibrated model had the greatest impact on mean daily flow rather than peak discharge. The

best model at Wilson is likely some combination of the models with and without channel infiltration, though the actual channel infiltration rate in the field is not known.

Incorporation of channel infiltration improves the plausibility of model parameters at Wilson, in particular the value of the loss to deep groundwater (DEEPFR). DEEPFR in the calibrated model without channel infiltration (0.9) was significantly higher than both the highest recommended value (0.2) and the "highest possible" value (0.5) (United States Environmental Protection Agency, 2000). The DEEPFR parameter should generally not exceed 0.4, and in other HSPF applications in San Diego County, DEEPFR was 0.1 (Tetra Tech, 2010). However, the Wilson Creek Tributary watershed is small, where losses to deep groundwater through either hillslope losses or channel infiltration might be more significant than in larger watersheds. Similarly, the infiltration rate (INFILT) and soil moisture storage (LZSN) were at the upper recommended range in the model without channel infiltration, and were higher than might be expected for bare surfaces, which at Wilson included bedrock outcrops that should have very limited infiltration rates and low or zero soil moisture storage. Inclusion of channel infiltration allowed reduction of DEEPFR, INFILT and LZSN to ranges that are closer to expected values, particularly for bare soil and rock.

Table 11. Parameter values describing infiltration (INFILT), lower zone soil moisture storage (LZSN), and groundwater recession rate (AGWRC) for the default SD11 and calibrated SD11 at Guejito (GUE) and Wilson (WIL). These parameters are contained in the PWAT-PARM2 block. The calibrated models are the same as the SD11G and SD11W series in Figures 6 to 14 and Tables 5-6.

DESCRIPTION			INFILT (Typical 0.01-0.25)			LZSN (Typical 3-8)			AGWRC (Typical 0.92-0.99)		
SOIL	COVER	SLOPE	SD11	GUE	WIL	SD11	GUE	WIL	SD11	GUE	WIL
C	Grass	Flat (0-5%)	0.050	0.078	0.078	4.8	4.8	6.8	0.920	0.935	0.935
C	Grass	Mod (5-10%)	0.040	0.072	0.072	4.5	4.5	6.5	0.920	0.935	0.935
C	Grass	Steep (10-20)	0.030	0.062	0.062	4.2	4.2	6.2	0.920	0.935	0.935
C	Dirt	Flat (0-5%)	0.045	0.048	0.048	4.8	4.8	6.8	0.950	0.935	0.935
C	Dirt	Mod (5-10%)	0.040	0.045	0.045	4.5	4.5	5.5	0.950	0.935	0.935
C	Dirt	Steep (10-20%)	0.030	0.040	NA	4.2	4.2	NA	0.950	0.935	NA
C	Gravel	Flat (0-5)	0.022	0.022	NA	2.4	2.4	NA	0.950	0.935	NA
C	Gravel	Mod (5-10)	0.020	0.020	NA	2.2	2.2	NA	0.950	0.935	NA
C	Gravel	Steep (10-20)	0.015	0.015	0.035	2.1	2.1	2.1	0.950	0.935	0.935
D	Grass	Flat (0-5%)	0.040	0.075	0.075	4.8	4.8	6.8	0.920	0.935	0.935
D	Grass	Mod (5-10%)	0.030	0.070	0.070	4.5	4.5	6.5	0.920	0.935	0.935
D	Grass	Steep (10-20)	0.020	0.060	0.060	4.2	4.2	6.2	0.920	0.935	0.935
D	Dirt	Flat (0-5%)	0.045	0.048	0.048	4.8	4.8	6.8	0.950	0.935	0.935
D	Dirt	Mod (5-10%)	0.040	0.045	0.045	4.5	4.5	5.5	0.950	0.935	0.935
D	Dirt	Steep (10-20%)	0.030	0.040	NA	4.2	4.2	NA	0.950	0.935	NA
D	Gravel	Flat (0-5)	0.022	0.022	NA	2.4	2.4	NA	0.950	0.935	NA
D	Gravel	Mod (5-10)	0.020	0.020	NA	2.2	2.2	NA	0.950	0.935	NA
D	Gravel	Steep (10-20)	0.015	0.015	0.035	2.1	2.1	3.1	0.950	0.935	0.935

Table 12. Parameter values in the PWAT.PARM3 block for the default SD11 and calibrated SD11 at Guejito (GUE) and Wilson (WIL), all without channel infiltration. The calibrated models are the same as the SD11cal series in Figures 6-14 and Tables 5-6.

	INFEXP	INFILD	DEEPFR (Typical 0-0.2)	BASETP (Typical 0-0.05)	AGWETP (Typical 0-0.05)
SD11	2.0000	2.0000	0.40	0.05	0.05
GUE	2.0000	2.0000	0.05	0.05	0.00
WIL	2.0000	2.0000	0.90	0.15	0.00

Table 13. Parameter values in the PWAT.PARM4 block for the default SD11 and calibrated SD11 at Guejito (GUE) and Wilson (WIL). The calibrated models are the same as the SD11cal series in Figures 6-14 and Tables 5-6.

DESCRIPTION			UZSN (Typical 0.1-1.0)			INTFW (Typical 1-3)			IRC (Typical 0.5-0.7		
SOIL	COVER	SLOPE	SD11	GUE	WIL	SD11	GUE	WIL	SD11	GUE	WIL
C	Grass	Flat (0-5%)	0.60	0.90	0.90	1.5	2.8	2.8	0.70	0.60	0.60
C	Grass	Mod (5-10%)	0.60	0.82	0.82	1.5	2.4	2.4	0.70	0.50	0.50
C	Grass	Steep (10-20)	0.60	0.78	0.78	1.5	2.2	2.2	0.70	0.40	0.40
C	Dirt	Flat (0-5%)	0.80	0.80	0.80	2.0	2.0	2.0	0.70	0.60	0.60
C	Dirt	Mod (5-10%)	0.70	0.50	0.50	1.2	1.8	1.8	0.45	0.45	0.45
C	Dirt	Steep (10-20%)	0.55	0.50	NA	0.8	0.9	NA	0.40	0.40	NA
C	Gravel	Flat (0-5)	1.60	1.60	NA	0.0	2.0	NA	0.70	0.60	NA
C	Gravel	Mod (5-10)	1.40	1.40	NA	0.0	1.8	NA	0.45	0.45	NA
C	Gravel	Steep (10-20)	1.10	1.10	1.10	0.0	0.9	0.9	0.40	0.40	0.40
D	Grass	Flat (0-5%)	0.60	0.90	0.90	1.5	2.8	2.8	0.70	0.60	0.60
D	Grass	Mod (5-10%)	0.60	0.82	0.82	1.5	2.4	2.4	0.70	0.50	0.50
D	Grass	Steep (10-20)	0.60	0.78	0.78	1.5	2.2	2.2	0.70	0.40	0.40
D	Dirt	Flat (0-5%)	0.80	0.80	0.80	2.0	2.0	2.0	0.70	0.60	0.60
D	Dirt	Mod (5-10%)	0.70	0.70	0.70	1.2	1.8	1.8	0.45	0.45	0.45
D	Dirt	Steep (10-20%)	0.55	0.55	0.55	0.8	0.9	0.9	0.40	0.40	0.40
D	Gravel	Flat (0-5)	1.60	1.60	1.60	0.0	2.0	2.0	0.70	0.60	0.60
D	Gravel	Mod (5-10)	1.40	1.40	1.40	0.0	1.8	1.8	0.45	0.45	0.45
D	Gravel	Steep (10-20)	1.10	1.10	1.10	0.0	0.9	0.9	0.40	0.40	0.40

Table 14. Runoff depth (inches) by hydrologic pathway for the SD11 model, both default (SD11) and calibrated (SD11G and SD11W) for soil type D, steep slopes (>10%).

	SD11 at Guejito			SD11G at Guejito			SD11 at Wilson		SD11W at Wilson	
	Grass	Dirt	Gravel	Grass	Dirt	Gravel	Grass	Gravel	Grass	Gravel
Surface	1.2	1.34	1.56	0.15	0.46	1.56	2.28	3.25	0.25	1.86
Interflow	0.77	0.30	0.00	0.67	1.05	1.53	1.19	0.00	1.02	0.65
Baseflow	0.16	0.23	0.18	0.64	1.1	0.68	0.45	0.59	0.09	0.12
Total Storm	1.97	1.64	1.56	0.82	1.51	3.09	3.47	3.25	1.27	2.51
Total	2.12	1.87	1.74	1.46	2.61	3.77	3.92	3.84	1.36	2.63

Discussion and Conclusion

The modeling shows that 1) the default parameters in SD08 significantly overpredict all aspects of the hydrograph, including annual discharge, discharge at all exceedence probabilities, and flows at

different recurrence intervals. 2) SD11 has significantly lower errors than SD08, despite its lumping of all vegetation into a single category (grass), with acceptable (<140%) errors in Q2-Q10, with the exception of high error (1200%) for Q2 in the small watershed (Wilson). 3) Q2 is particularly low and not well predicted by uncalibrated models, with overestimation of several folds for both SD11 and USGS regressions. Q5 and Q10 were predicted more accurately than Q2 by all models, but were underpredicted by USGS regressions. 4) Parameters for the calibrated models were different between the small watershed and large watershed, with higher groundwater loss rates and higher storage capacity in lower soil zones in the small watershed. However, the parameters from the model calibrated to the large watershed predicted Q5 and Q10 with acceptable accuracy (error < 50%). Note that the study watersheds were mostly on soil types C and D, so there remains limited information on model parameters for soil with higher infiltration capacities (groups A-B).

The large overprediction of Q2 by default model parameters was also found for an application of HEC-HMS to watersheds in San Diego County, including Guejito (Humphreys et al., 2013) (Table 15). Peak discharges of all recurrence intervals were over-predicted by the model, with the largest overprediction for Q2, with a mean prediction error of +2821% (Table 15). Q2 from both observations and the calibrated models are also much lower than from a previous implementation of SD11 for a hypothetical small watershed (Table 16) (Parra et al, 2012). Together, the comparison suggests that Q2 is much lower than expected from both SD11 and from other models in San Diego.

Table 15. Modelled and predicted peak discharges (cfs) for six watersheds in San Diego County using the HEC-HMS model. Imp indicates the percentage impervious surface. Adapted from Table 2 in Humphreys et al. (2013).

	Guejito 22.5 mi^2 Imp. 8%			Jamul Creek 70.1 mi^2			Las Flores Creek 26.6 mi^2 Imp. 10%		
	HEC-HMS	Obs.	%Δ	HEC-HMS	Obs.	%Δ	HEC-HMS	Obs.	%Δ
Q10	7447	1040	+616%	15,218	2240	+579%	4250	2240	+90%
Q5	5756	467	+1132%	13,899	975	+1326%	3344	975	+243%
Q2	4146	98	+4130%	8,058	166	+4754%	1588	166	+857%
	Los Coches Creek 12.2 mi^2 Imp 19%			Santa Maria Creek 57.0 mi^2			Sweetwater River 44.5 mi^2		
	HEC-HMS	Obs.	%Δ	HEC-HMS	Obs.	%Δ	HEC-HMS	Obs.	%Δ
Q10	2894	572	+406%	7684	2410	219%	14479	2580	+461%
Q5	2459	386	+537%	6058	968	526%	11788	1040	+1033%
Q2	1535	173	+787%	3633	146	2388%	7603	185	+4010%

Table 16. Observed and modelled Q2 for Guejito, Wilson, including a comparison with HEC-HMS implemented at Guejito in Humphreys et al (2013), and with a theoretical small watershed on C-type soils presented in Parra et al (2012).

	Q2, cfs/acre	Source
Wilson (annual max series, 15-min)		
Observed	0.012	This study
SD08	0.192	This study
SD11	0.135	This study
SD11W	0.016	This study
USGS2012	0.052	This study
Guejito (annual max)		
Observed	0.007	Humphreys et al, 2013
HEC-HMS	0.288	Humphreys et al, 2013
Observed, 1966-1981	0.006	This study
SD08, 1966-1981	0.071	This study
SD11, 1966-1981	0.009	
SD11G, 1966-1981	0.004	This study
USGS2012, 1966-1981	0.020	This study
10 acre watershed, Lake Wohlford Station Slope 5 degrees, Soil C		
SWMM (partial duration, hour)	0.284	Parra et al, 2012
SDHM (partial duration, hour)	0.204	Parra et al, 2012

Model parameter interpretation and hydrologic pathways

The SD11 parameters required adjustment, both for fitting observed flows as well as to be more consistent with physical hydrological processes. For example, most parameters relating to soil

properties (infiltration capacity, soil moisture storage, interflow) do not vary between grass and dirt, which is contrary to field studies showing strong impacts of vegetation on infiltration rates and other soil properties (Dunne and Leopold, 1978). Varying soil parameters by land cover type will likely result in better model fits as well as providing more realistic assessments of the impact of urbanization on watershed hydrology.

The groundwater loss parameter suggests that channel infiltration or other subsurface losses may be an important process, particularly in small watersheds. In the smallest watershed (Wilson) accurate predictions of daily runoff were only possible by assuming high values for the groundwater loss parameter (DEEPFR), while SD11G used acceptable values of DEEPFR, suggesting that channel infiltration may be less important in large watersheds where the infiltrated water may contribute to baseflow later in the storm or season. In a model without channel infiltration, it is possible that high DEEPFR parameters are necessary to reproduce observed hydrologic behavior in small watersheds San Diego County.

Runoff production from different surfaces in the default SD11 model is not consistent with field observations. SD11 predicts that more runoff is generated from grass than from dirt or gravel, which is not found in field studies, where grass and other vegetation increase infiltrations rates and evapotranspiration, reducing total storm and total annual runoff at both the plot scale (Gutierrez and Hernandez, 1996) and the hillslope scale (Bartley et al., 2006). Similar patterns are observed in watersheds with chaparral, where removal of chaparral increases stormflow and runoff, though the effect may be modest for locations with low rainfall (<18 inches) (Hibbert, 1983). Since no land cover change was observed during the period of record, the impact of land cover on runoff can only be inferred from model parameters, and remains uncertain.

Parameter uncertainty

Channel geometry and water storage in the channel may have large impacts on modelled peak discharge, but the actual channel parameters are not well constrained, in particular the channel length and channel geometry at the channel head. Even in a small watershed (Wilson), several tributary channels were not represented in the model, which may cause error in predicted peak discharge. Future modeling efforts to predict peak discharges need to pay close attention to channel geometry, roughness, and stage-volume-discharge relationships as represented in the FTABLES.

Precipitation data used to calibrate the models was somewhat uncertain given the distance from the stations to the watersheds, particularly for Guejito. Future modeling work could incorporate radar-based precipitation estimates for more accurate determination of precipitation rates.

Management implications

While SD11 predicts Qx with acceptable accuracy in the large watershed, Qx was overpredicted in the small watershed, which is the scale at which most modeling for HMP compliance occurs. Q2 in particular is overpredicted by the default SD11 model in the small watershed. The parameters in SD11 are derived from other studies of much larger watersheds and/or watersheds with mixed land uses and soil types, which complicates accurate identification of parameters for natural or reference conditions. While it is expected that a calibrated model would outperform an uncalibrated model, and while the developers of the SDHM accurately note that the default parameters in SDHM are meant as a starting point for calibration, in practice SDHM is used as a management tool in San Diego without additional calibration due to limited data availability at specific sites. The uncalibrated SDHM overpredicts

discharge and Qx at both study watersheds, which suggests that revisions of the parameters in SDHM may be necessary to provide reasonably accurate predictions of discharge for ungaged watersheds in San Diego County.

Inclusion of channel infiltration may more accurately represent the hydrological processes, which could be important for prediction of the impact of urbanization on runoff. For example, if hillslopes produce high volumes of water but channel infiltration is high, as in the calibrated Wilson model with channel infiltration, then development may have less of an impact on runoff than if hillslopes produce little runoff, as in the Wilson model without channel infiltration.

The current modeling effort did not include urban vegetation or impervious surfaces. Future modeling efforts should focus on applying the model to urbanized watersheds in order to more accurately parameterize the model under urban conditions. Additional modeling should also consider the impact of uncertainty in model parameters on predicted peak discharges, and would ideally provide a range of possible values for peak discharges at a range of recurrence intervals.

References

Abrahams, A.D., Parsons, A.J., 1991. Relation between infiltration and stone cover on a semiarid hillslope, southern Arizona. J. Hydrol. 122, 49–59. doi:http://dx.doi.org/10.1016/0022-1694(91)90171-D

Ackerman, D., Schiff, K.C., Weisberg, S.B., 2005. Evaluating HSPF in an arid, urbanized watershed. J. Am. Water Resour. Assoc. 41, 477–486. doi:10.1111/j.1752-1688.2005.tb03750.x

AQUA TERRA, 2006. Hydrologic Modeling of the Castro Valley Creek and Alameda Creek Watersheds with the US EPA Hydrologic Simulation Program–FORTRAN, Final Report. Prepared for the Alameda Countywide Clean Water Program, Hayward, CA. Mountain View, CA, USA.

AQUA TERRA, 2005. Hydrologic Modeling of the Calleguas Creek Watershed with the US EPA Hydrologic Simulation Program–FORTRAN, Final Report. Prepared for the Ventura County Watershed Protection District, Ventura CA. Mountain View, CA, USA.

Bartley, R., Roth, C.H., Ludwig, J., McJannet, D., Liedloff, A., Corfield, J., Hawdon, A., Abbott, B., 2006. Runoff and erosion from Australia's tropical semi-arid rangelands: influence of ground cover for differing space and time scales. Hydrol. Process. 20, 3317–3333.

Bekele, T., Simon, E., Baryohay, D., Kent, F., 2005. Comparison of Some Reference Evapotranspiration Equations for California. J. Irrig. Drain. Eng. 131, 73–84.

Bicknell, J., Beyerlein, D., Feng, A., 2006. The Bay Area Hydrology Model – A Tool for Analyzing Hydromodification Effects of Development Projects and Sizing Solutions, in: California Stormwater Quality Association (CASQA) Conference. Sacramento, CA.

Brakensiek, D.L., Rawls, W.J., 1994. Soil containing rock fragments: effects on infiltration. CATENA 23, 99–110. doi:http://dx.doi.org/10.1016/0341-8162(94)90056-6

Cerdà, A., 2001. Effects of rock fragment cover on soil infiltration, interrill runoff and erosion. Eur. J. Soil Sci. 52, 59–68.

Clear Creek Solutions, 2012. South Orange County Hydrology Model Guidance Document, San Diego Region. Olympia, WA.

Dunkerley, D., 2000. Hydrologic effects of dryland shrubs: defining the spatial extent of modified soil water uptake rates at an Australian desert site. J. Arid Environ. 45, 159–172.

Dunne, T., Leopold, L.B., 1978. Water in Environmental Planning. W.H. Freeman and Company, New York.

Fierer, N.G., Gabet, E.J., 2002. Carbon and nitrogen losses by surface runoff following changes in vegetation. J. Environ. Qual. 31, 1207–1213.

Gotvald, A.J., Barth, N.A., Veilleux, A.G., Parrett, C., 2012. Methods for Determining Magnitude and Frequency of Floods in California, Based on Data through Water Year 2006. Reston, VA. doi:Scientific Investigations Report 2012-5113

Grant, W.J., Struchtemeyer, R.A., 1959. Influence of the coarse fraction in two Maine potato soils on infiltration, runoff and erosion. Soil Sci. Soc. Am. J. 23, 391–394.

Guay, J.R., 2002. Rainfall-Runoff Characteristics and Effects of Increased Urban Density on Streamflow and Infiltration in the Eastern Part of the San Jacinto River Basin, Riverside County, California. US Department of the Interior, US Geological Survey.

Gutierrez, J., Hernandez, I.I., 1996. Runoff and interrill erosion as affected by grass cover in a semi-arid rangeland of northern Mexico. J. Arid Environ. 34, 287–295. doi:http://dx.doi.org/10.1006/jare.1996.0110

Hawley, R.J., Bledsoe, B.P., 2011. How do flow peaks and durations change in suburbanizing semi-arid watersheds? A southern California case study. J. Hydrol. 405, 69–82.

Hibbert, A.R., 1983. Water yield improvement potential by vegetation management on western rangelands. J. Am. Water Resour. Assoc. 19, 375–381. doi:10.1111/j.1752-1688.1983.tb04594.x

Humphreys, S., Mohrlock, C., Cooper, D., Paquette, J., Beighley, R.E., Barry, A., 2013. Analysis of results for the County of San Diego Rainfall Distribution Study Project. San Diego, CA.

Lu, J., Sun, G., McNulty, S.G., Amatya, D.M., 2005. A comparison of six potential evapotranspiration methods for regional use in the southeastern United States. J. Am. Water Resour. Assoc. 41, 621–633.

Martin, D.A., Moody, J.A., 2001. Comparison of soil infiltration rates in burned and unburned mountainous watersheds. Hydrol. Process. 15, 2893–2903.

Matlock, W.G., 1965. The effect of silt-laden water on infiltration in alluvial channels. The University of Arizona.

Niswonger, R.G., Prudic, D.E., Pohll, G., Constantz, J., 2005. Incorporating seepage losses into the unsteady streamflow equations for simulating intermittent flow along mountain front streams. Water Resour. Res. 41.

Poesen, J., Ingelmo-Sanchez, F., Mucher, H., 1990. The hydrological response of soil surfaces to rainfall as affected by cover and position of rock fragments in the top layer. Earth Surf. Process. Landforms 15, 653–671.

Ponce, V.M., Pandey, R.P., Kumar, S., 1999. Groundwater recharge by channel infiltration in El Barbon basin, Baja California, Mexico. J. Hydrol. 214, 1–7. doi:10.1016/S0022-1694(98)00220-0

RBF Consulting, 2013. Santa Margarita Region Hydromodification Management Plan.

Scanlon, B.R., Keese, K.E., Flint, A.L., Flint, L.E., Gaye, C.B., Edmunds, W.M., Simmers, I., 2006. Global synthesis of groundwater recharge in semiarid and arid regions. Hydrol. Process. 20, 3335–3370. doi:10.1002/hyp.6335

Stallcup, J.A., White, M.D., Staus, N.L., Spencer, W.D., 2005. Conservation Significance of Rancho Guejito. San Diego, CA.

Tetra Tech, 2011. Hydromodification Software, Third Party Review. Research Triangle Park, NC.

Tetra Tech, 2010. Los Peñasquitos Lagoon Sediment TMDL Modeling - Final. San Diego, CA.

United States Environmental Protection Agency, 2000. BASINS Technical Note 6: Estimating Hydrology and Hydraulic Parameters for HSPF. Washington, D.C.

Waananen, A.O., Crippen, J.R., 1977. Magnitude and frequency of floods in California. Water Resources Division, US Geological Survey; available through the National Technical Information Service,.

Wilcox, B.P., Wood, M.K., Tromble, J.M., 1988. Factors Influencing Infiltrability of Semiarid Mountain Slopes. J. Range Manag. 41, 197–206. doi:10.2307/3899167

Yair, A., Lavee, H., 1976. Runoff generative process and runoff yield from arid talus mantled slopes. Earth Surf. Process. 1, 235–247.

ESA

550 Kearny Street
Suite 800
San Francisco, CA 94108
415.896.5900 phone
415.896.0332 fax

www.esassoc.com

memorandum

date June 13, 2014

to Stuart Kuhn and René Vidales, County of San Diego, Watershed Protection Program

from Brian Haines and Andy Collison

subject Remote sensing of monitoring sites to document historical channel evolution and potential future trajectories (Weston Contract 534965, Hydromodification Monitoring Services add-on, Task 1)

Introduction

Small ephemeral headwater channels are subject to large inter-annual variations in precipitation and runoff and are sensitive to changes in land use within the contributing watershed. Channels respond to changes in runoff and sediment supply by adjusting their physical form. These adjustments may occur over varied timespans ranging from a few hours to a several years depending on watershed conditions and the nature of driving events. While existing HMP monitoring elements – channel surveys and geomorphic assessments - are documenting channel form in the short-term, little is known about the historical form and long-term evolution of the receiving channel. Historic aerial photography and topographic maps can be used to document variations in channel form over time, and can help identify landscape altering events, natural or anthropogenic, which may have contributed to contemporary channel form.

The San Diego Copermittees identified "remote sensing" of HMP monitoring sites as a medium priority addition in the 2013 re-evaluation of the monitoring plan. The County of San Diego issued a task order to ESA under the Weston reporting contract to conduct the remote sensing work for the 9 existing HMP sites (Table 1). The purpose of this memorandum is the document the remote sensing process, which includes historical reconstructions of watershed events and receiving channel changes using aerial photography and topographic maps. The primary goals of the remote sensing task are to improve our understanding of the long-term drivers and historical trajectories of channel response and to predict potential future responses.

Existing Conditions of Monitoring Sites

The remote sensing analysis was conducted on nine (9) receiving channels, which were screened, assessed, and secured for monitoring as part of the HMP effective assessment monitoring project (Figure 1). These monitoring sites are comprised of the following types:

- 3 Development sites – cross-sections of receiving channels downstream of future development projects
- 4 Reference sites – selected channel cross-sections within relatively undeveloped watersheds
- 2 Urban sites – selected cross-sections downstream of already developed watersheds

Each monitoring site has a unique receiving channel and susceptibility to hydromodification ranging from MEDIUM to HIGH based on the SCCWRP screening tool classifications and low flow calculator. Baseline

channel assessments and surveys documented the existing condition of the receiving channel and contributing watershed. Repeat annual assessments and surveys have documented channel changes over the past 2-3 years depending on when the monitoring site was secured. A summary of existing conditions has been provided in Table 1.

Table 1. Existing condition of monitoring sites.

Site ID	Monitoring Site	Type of Site	Susceptibility to Hydromodification	Existing Condition
DH-1	Otay Village	Development	HIGH	Incised, but relatively stable cobble-bed channel confined by adjacent hillslopes. Watershed was burned by the Otay Fire of 2003. Channel base level is governed by water levels in Otay Lake.
DH-2	Bear Valley	Development	HIGH	Aggrading sand-bed channel set in a broad alluvial valley. Upstream channel erosion due to culvert. Watershed is partially developed.
DH-3	MDS	Development	HIGH	Incised sand-bed channel located on an alluvial fan at the mouth of a steep confined canyon. Small headcuts observed downstream during field assessments.
RM-1	Deer Valley	Reference	MEDIUM	Stable cobble-bed channel within a narrow valley with partial hillslope confinement. Watershed is undeveloped and used as recreational open space.
RM-2	Sycamore Canyon	Reference	MEDIUM	Unstable mixed-bed channel (sand and gravel) with connected floodplain. Undeveloped watershed with prior ranching. Channel is recovering from Cedar Fire of 2003.
RH-1	Ramona Grasslands	Reference	HIGH	Incised, but stable sand-bed channel within a relatively confined valley. Long-term cattle grazing and Witch Creek Fire of 2007 have affected the watershed setting.
RH-2	Schoolhouse Canyon	Reference	HIGH	Unstable sand-bed channel on an alluvial fan near the mouth of a steep confined canyon. Watershed is still responding to the Witch Creek Fire of 2007.
UM-1	Flanders Canyon	Urban	MEDIUM	Recovering cobble-bed channel with broad well connected floodplain. Upstream hydromodification and channel erosion.
UH-1	Saratoga	Urban	HIGH	Unstable sand-bed channel in a confined valley. Hydromodification and urban base flow. Severe channel erosion upstream of site. Failing grade control downstream.

Remote Sensing Methods

Topographic maps and aerial photography were used to reconstruct the historical condition of each monitoring site. The domain of analysis included the contributing watershed and downstream limit of the receiving channel based on guidance provided in the SCCWRP hydromodification screening tools field manual (e.g. downstream grade control or doubling of contributing watershed area; Bledsoe et al. 2010). The contributing watersheds were delineated using the California StreamStats Interactive Map (USGS 2014). A total of 33 georeferenced topographic maps and aerial images were selected and purchased to span the available historical record of the sites. Historical imagery was purchased through the NETR Online resource (NETR 2014). More modern imagery was extracted from Google Earth Pro (Google 2014).

Each map and image was closely examined to identify changes in land use, the occurrence of major watershed events, and changes in receiving channel. Some examples include:

- The conversion of agricultural land to suburban residences

- Changes in vegetation coverage and sediment delivery post-wildfire
- Channel relocation and channelization
- Channel widening and braiding
- Disturbance and recovery of riparian vegetation after flood events

Channel and valley measurements such as top width and sinuosity were recorded where relevant. To the extent possible, the channel evolution model for Southern California (Hawley et al. 2012) was used to reconstruct the historical evolution of the receiving channel based on observed watershed drivers (e.g. increased sediment supply from the basin due to wildfire) and changes in channel form (e.g. widening and braiding of channel then recovery to a single thread channel). Predictions of future channel changes were made based on the existing channel evolution stage, historic trajectory of channel changes, expected future watershed condition, and watershed management considerations.

Historical Channel Assessments

For each of the monitoring sites listed below, a small narrative has been provided outlining the watershed history and current condition based on observable changes in land use, vegetative cover, and channel morphology. Supporting figures for each site – select time-series of topographic maps, historic aerial photography, and oblique imagery – are included as an attachment at the end of the memorandum.

DH-1, Otay Village

The Otay Village watershed upstream of the monitoring site has remained relatively unchanged since the earliest topographic maps in 1912, and has been subject to few significant human-caused changes. The dominant land use of the watershed is open space and the first aerial photos in 1953 show grazed land with some light scrub (Figure Set 1). There is a stock pond on the creek upstream of the monitoring site which may have trapped sediment and had some effect on the creek evolution. The creek is hard to see in detail on aerial photos but no major changes have been observed.

The main watershed changes around the site include the construction of the Lower Otay Reservoir in 1918 which may have affected base level in the creek inducing aggradation in the lowest reach. Changes in water level during wet and dry years may have caused small waves of incision and aggradation in the lowest reach. The most recent watershed change appears to have been the Otay Fire of 2002 that scorched areas of scrub upstream of the site. No morphological response was visible in the aerial photos from this event.

DH-2, Bear Valley

The earliest maps of Bear Valley (1893) show open ground, but by 1901 a well-developed road network had been built, presumably serving the agricultural field and orchard system near Escondido (Figure Set 2). Little change in the watershed was visible until 1964, when houses started to appear along the existing road network. By 1964 the suburbs of Escondido expanded from the north into the Bear Valley watershed; The road network was improved, and the first subdivisions appeared. From 1968 to 1978 subdivisions expanded southward, closer to the monitoring site. Most of the existing urbanization present today in the west side of the watershed had occurred by 1978, with additional infill occurring on the east side since 1980.

The land use close to the monitoring site was primarily orchards by 1947 and return flows from the orchard and the culvert underneath Idaho Road to the north appears to have played a role in the stability and evolution of the receiving channel. The creek upstream of Idaho Road was channelized, and downstream the creek expanded into a broad swale with potential erosion pathways up to 150 feet in width (though this isn't entirely clear from the imagery). By 1964, portions of the upstream watershed were culverted as housing replaced orchards, and sections of the remaining creek were channelized and appeared to have been maintained for stormwater conveyance.

Upstream of Idaho Road the creek had expanded into a broad, highly eroded channel, and downstream sedimentation and revegetation had narrowed the channel corridor near the monitoring site.

Long-term water ponding downstream of the monitoring site encouraged growth of an isolated (not contiguous) riparian area, which appears in 1980 and is quite dense by 2013. The riparian area acts as a form of downstream grade control and has played an important role in maintaining the existing form of the receiving channel at the monitoring site. Channel erosion upstream of the monitoring site has triggered small episodes of cut and fill at the monitoring site, but no major channel changes have been observed since 1994.

DH-3, MDS Development

The contributing watershed of the MDS Development was ranched land from the first topographic map in 1903 until orchards were developed on the slopes closest to the monitoring site by the 1989 aerial photo (Figure Set 3). A few access roads including Paseo Tranquil Lane expanded into the headwaters during this time, and by 1994, lots were being cleared for development of single family homes. Historical cattle grazing and irrigation return flows from the orchards likely led to erosion and sedimentation of the receiving channel though this impact is hard to document from the imagery. In 2003, low density residential development started in the headwaters of the creek, continuing to the present. Today approximately half of the residential lots remain vacant, and the proportion of impervious land within the watershed is relatively low (in contrast with concurrent development along Black Canyon Road downstream of the site).

The most notable watershed event occurred sometime in 2005, a year associated with major storm events in the San Diego region. Sediment deposition in the creek was apparent in the 2005 image, and a large sediment plume was observed at the mouth of canyon near Lapis Lane. Prior to 2005, the creek at the monitoring site was approximately 5 to 10 feet wide, but the creek widened up to 30 feet in response to the severe deposition. Imagery from 2006 to 2012 shows that the creek narrowed to approximately 12 feet in width as sediment was flushed from the system and grasses and riparian vegetation reestablished the floodplain. Today the creek averages 4 feet in width near the monitoring site.

RM-1, Deer Valley

The Deer Valley site does not appear to have undergone any significant watershed change in the last 100 years. Topographic maps from 1903 show the watershed as open space with no houses or trails. The watershed appears to have remained with dense scrub on the north facing slopes and slightly sparser scrub on the south facing slopes since the first aerial photo in 1953, with a single trail along the watershed divide in the headwaters (Figure Set 4). A small foot trail appeared along the north side of the creek between 2008-09. There have been no land use changes that would be expected to cause a channel response.

The detailed channel morphology is not visible in the aerial photos or topographic maps, and no changes can be discerned from the data available. Field observations suggest that the channel is stable under existing conditions, and has as Medium susceptibility to hydromodification.

RM-2, Sycamore Canyon

The earliest maps for Sycamore Canyon (1916) shows the Goodan ranch house but no other development in the watershed. The first aerial photos in 1953 show the watershed with a mixture of scrub and grazed areas, with some areas appearing to oscillate between grazed and scrub on successive aerials (Figure Set 5). A stock pond can be seen downstream of the monitoring site. The only development in the watershed is road construction associated with the San Diego Aqueduct, which crosses Sycamore Creek downstream of the monitoring site, and a public access road, which leads to a staging area and trailhead for the open space preserve. In 2003 the watershed was burned by the Cedar Fire, evidence of which can be seen in the aerial images with loss of ground vegetation.

Oblique images of the creek before the fire show a scrubby riparian corridor, with widespread loss of vegetation following the fire. Imagery from June 2005 shows the channel at the monitoring site widening from 15 feet to 42 feet and aggrading post-fire, presumably due to a combination of loss of bank resistance from the burned vegetation and high runoff and watershed erosion associated with the 2005 storm events. In subsequent years we can see vegetation reestablishing in the riparian corridor, colonizing the bars deposited around the monitoring site, and causing the channel to narrow to around 10 feet.

RH-1, Ramona Grasslands

The Ramona site does not appear to have undergone much watershed land use change in the last 100 years. Topographic maps from 1909 show the watershed as open ground with no houses and few trails. The creek forms a divide between two land covers that have largely persisted since the 1953 aerial photo: grazing on the north side of the creek and fallow land / scrub-oak savannah on the south valley side (Figure Set 6). A small portion of the headwaters on the mesa was scrub in 1971 and had been cleared to create orchards by 1980. Between 1996 and 2002 the upper headwater (approximately 10% of the total watershed area) had been converted from orchards and scrub to vineyards and a winery (seen in the 2003 image).

The largest, most recent disturbance in the watershed has been the Witch Creek Fire of 2007. Images pre and post-fire show the scrub on the south side of the creek having burned off, leaving bare ground and erosion features visible in the 2008 aerials. The ground cover appeared to recover within 1-2 years and now resembles pre-fire cover.

The channel is very small (approximately a 2-foot bottom width) and cannot be seen clearly in aerial imagery. Therefore, little can be directly observed about channel morphology or long-term evolution. Most of the channel is incised and has a ‘High’ susceptibility to hydromodification, but there are localized areas of natural granite bedrock and boulders that act as grade control and bank protection.

RH-2, Schoolhouse Canyon

The north fork of Schoolhouse Canyon has remained largely undeveloped since the first topographic maps were available in 1903. The south facing valley side has remained sparsely vegetated throughout the period for which images are available, while the north facing slopes have displayed a mix of grasses and light scrub (Figure Set 7). The south fork was undeveloped until around 1984, when the first low density housing sites began to appear on the aerial photos. Development occurred between the 1980s and 1994, by which time around 15-20 large houses had been constructed near the watershed divide.

The watershed of Schoolhouse Canyon was also burned during the Witch Creek Fire of 2007. Aerial photos from 2008 show the ground almost completely denuded of vegetation, and reveal soil creep terracettes on the south valley side that indicate historic grazing of watershed. Vegetation had recovered to pre-fire levels by about 2012. The response of the receiving channel to the fire was evident in aerial imagery from 2008 to 2009 where the channel expanded from 10 feet to 40 feet in width as sediment was washed during storm events from the upper watershed and deposited in the lower reaches of the canyon. Subsequent storm events have washed sediment from the canyon into sediment basins further downstream, and bed incision and floodplain revegetation have narrowed the active channel width to 13 feet.

UM-1, Flanders Canyon

The earliest topographic maps for the watershed show Flanders Canyon as ranchland in 1903 with a few dirt roads and almost no buildings. This was still the case in 1953 when the first aerial photos were taken (Figure Set 8). The 1953 aerial photos show the ephemeral creek in Flanders Canyon as a narrow, slightly sinuous single channel

with a scrub dominated floodplain. The well-defined canyon portion of the creek extended about a mile upstream of its current above-ground limit at Flanders Drive and Parkdale Avenue. By 1964 the current major road network and some limited subdivisions were under construction in what became Mira Mesa, located in the headwaters of Flanders Canyon. The creek planform looked largely as it had in 1953, with a little more scrub on the floodplain suggesting that the creek was laterally stable and the floodplain had not been actively scoured since the last aerial photos. Between 1964 and 1972 about half of Mira Mesa, making up most of the headwaters of the creek, had become urbanized and the upper 3,000 feet of the creek had been culverted and converted to a stormdrain as development pads were built over the canyon. We infer that the stormdrain network in Mira Mesa keys into this culvert, effectively increasing the drainage density into the creek at this location in addition to the large increase in impervious area. By 1980 most of Mira Mesa had been urbanized, development had spread from the headwaters down the mesa to the middle reaches of canyon, and more than 4,700 feet of channel had been culverted and buried. Between 1980 and 1989 urbanization extended downstream and the mesa above lower Flanders Canyon was developed to about its current limits.

The first downstream channel response is visible in the 1980 aerial photos, with the channel approximately doubling in width between Kaufman Way (half a mile upstream of Camino Santa Fe) and El Camino Memorial Park near Fenton Road. Grading associated with the construction of Camino Santa Fe and the surrounding area directly impacted the creek near the monitoring site between 1980 and 1989, and the channel doubled in width again in some locations (~55 feet in width at the monitoring site). Development of a fill pad on the southern side of the canyon created an alluvial fan upstream of the monitoring site that contributed to channel widening downstream (visible in the 1994 Google Earth image). The date in not known in detail, but a sewer line was constructed in a trench in the channel, presumably associated with the construction of Camino Santa Fe. Between 1994 and 2005 the channel narrowed and the floodplain became more vegetated as the creek equilibrated from the pulse of sediment generated by development. The 2005 flood appears to have widened some reaches of the channel near the monitoring site. Some localized bank erosion and widening was visible following the 2010 flow event. Since 2005 the channel appears to have relatively stable dimensions, while the floodplain continues to become more vegetated.

UH-1, Saratoga

In 1893 (the date of the first available USGS topographic map) what is now the core of the City of Escondido was established down to about 8th Avenue, and the mesa portion of the headwaters of Saratoga Creek were laid out in a field system with some roads but few buildings or impervious areas. The valley sides draining directly into the creek appear to have been grazed or unused. Saratoga Creek is indicated as an ephemeral channel with a dashed blue line. After World War II the field system expanded into more of the headwaters area west of the creek, but with little urban development. Between the early 1960s to 1970 Escondido started rapidly expanding south into the headwaters of Saratoga Creek for the first time, developing former field areas and likely extending the density and efficiency of the drainage network. In addition to dense development in the headwaters, low density houses started to be constructed in the watershed around the creek at this time. This was probably the first major hydromodification phase affecting Saratoga Creek. A second large wave of urban expansion occurred in the 1980s, which included development on the formerly undeveloped valley sides close to Saratoga Creek, through the creek retains a 150-200 ft wooded riparian corridor. During the 1980s the reach of Saratoga Creek upstream of South Escondido Boulevard appears to have been converted from an open channel with a narrow riparian corridor to a culverted system. The second major phase of hydromodification was probably more significant than the first due to its proximity and effect on the upstream drainage network.

The maps and aerial photos do not reveal Saratoga Creek directly, though downstream of Escondido Boulevard it has had a well-developed and persistent riparian corridor since the first aerial photos in 1947. As a result no morphological observations can be made from these sources. However, field observations show Saratoga Creek to be deeply incised and widened upstream of the monitoring site (~ 40 feet wide and 20 feet deep) where grade control is not present, and it is inferred that this incision started in the 1960s and was reinvigorated in the 1990s.

Grade control downstream of the monitoring site at Las Palmas Road has kept the lower portion of the creek relatively stable in comparison to the upstream reaches, though headcuts have migrated upstream through the site, banks have eroded slightly, and some trees have fallen into the channel. It is likely that the well vegetated banks, root growth into the bed of the creek, and partially cohesive soils have also slowed erosion in the lower reaches.

Potential Future Channel Reponses

The expected future watershed condition and existing channel condition were the primary considerations in predicting future channel response. Because the future watershed condition is dependent on management actions, potential channel responses have been analyzed with and without important watershed management considerations (Table 2). In addition, the following notes provide for potential future channel responses on five of the sites:

DH-3 MDS Development - There is potential for the ongoing development in the headwaters to trigger a second round of channel enlargement, though grade control in the form of a culvert under Lapis Lane may limit vertical incision in the lower reach.

RH-1 Ramona Grasslands - Because the existing level of development is relatively low (1% impervious cover, approximately 10% vineyard and associated land use) we do not expect significant anthropogenic change in the channel. However, the somewhat confined nature of the channel and the 'High' susceptibility of the channel creates the risk of channel incision if further vineyard development occurs upstream.

RH-2 Schoolhouse Canyon - The detailed channel morphology is not visible in the aerial photos or topographic maps, and no changes can be discerned from the data available. It is likely that the 2007 fire generated a pulse of sediment that may find its way down the channel and aggrade near the monitoring site, where the valley gradient flattens. We might expect the channel to adjust over time and incise back through this aggraded sediment to restore the original channel form. Continued development in the upper watershed could increase runoff and generate channel erosion.

UM-1 Flanders Canyon - At this point the channel appears to be in relative equilibrium with its watershed. This creek has a very high coarse sediment yield from the canyon side slopes, and it is possible that prior to hydromodification the creek was transport limited (received more sediment supply from the valley sides and bank erosion than it could transport). One hypothesis is that the remaining sediment supply is sufficiently abundant and coarse that the increasing water supply and reducing sediment have not pushed the creek into a supply-limited condition, supporting stability. If this is the case we would expect the creek to be dynamically stable, meaning it would migrate and periodically widen in response to flood event (as seen in 2005) but that floodplain vegetation would recolonize and stabilize the creek after such events, causing the creek to narrow and recover its original form. At this stage the watershed is largely built out and future developments should comply with the HMP, so we would not expect a great change in watershed hydrology.

UH-1 Saratoga - We therefore expect the channel to persist in an unstable and confined state until a series of large events overcome bank strength and allow the system to widen into a more stable configuration. This condition could also be achieved through restoration/mitigation efforts.

Our assessment of potential channel responses does not directly consider future natural watershed disturbances such as flood events, drought, and wildfire.

Table 2. Potential future channel responses given watershed management considerations.

Site ID	Monitoring Site	Watershed Management Considerations	Potential Future Channel Responses	
			Without Management	With Management
DH-1	Otay Village	Ensure hydromod mitigation, and monitor reservoir water levels	Potential incision and widening from lake to culvert	Channel will likely maintain current form
DH-2	Bear Valley	Ensure hydromod mitigation from road expansion, and energy dissipation downstream of Idaho Ave	Continued erosion of upstream parcel and sedimentation at the monitoring site	Gradual recovery of upstream channel, channel at site may remain roughly the same
DH-3	MDS	Ensure hydromod mitigation, monitor any changes in road/culvert configuration at Lapis Lane	Continued cycles of significant erosion and sedimentation at mouth of canyon	Gradual recovery of channel with minimal cycles of channel cut and fill
RM-1	Deer Valley	Leave as open space, enforce use of trails to protect creek	Development may induce hydromodification and channel erosion	Channel will likely maintain current form
RM-2	Sycamore Canyon	Leave as open space, remove stock pond, and restore historic channel	Continued sedimentation in stock pond and downstream channel erosion	Gradual flush of sediment from system, recovery of upland and riparian vegetation, return to single thread channel
RH-1	Ramona Grasslands	Limit headwater development, keep remainder as open space, limit cattle access to channels.	Development may induce hydromodification and channel erosion. Grazing may induce bank erosion.	Channel will likely maintain current form
RH-2	Schoolhouse Canyon	Limit headwater development, keep remainder as open space, carefully manage downstream sediment basins and culverts.	Erosion and sedimentation of receiving channel (uncertain based on combination of management options).	Gradual recovery to a single-thread channel with occasion cycles of cut and fill.
UM-1	Flanders Canyon	Promote voluntary stormwater control programs (e.g. rain barrels, bioretention, etc.), limit channel modifications from sewer maintenance.	Continued cycles or erosion, sedimentation, and channel braiding.	Gradual recovery to a single-thread channel with occasion cycles of cut and fill
UH-1	Saratoga	Promote voluntary stormwater control programs (e.g. rain barrels, bioretention, etc.), repair downstream grade control, and assess opportunities for creek restoration.	Continued erosion from hydromodification. If grade control fails, severe erosion of channel near monitoring site and loss of park land.	Channel at monitoring site will maintain current form, potential recovery of upper watershed with extensive stormwater mitigation and channel restoration.

References

Bledsoe, B.P., Hawley, R.J., Stein, E.D., Booth, D.B., 2010. Hydromodification screening tools: field manual for assessing channel susceptibility. Technical report 606. Southern California Coastal Water Research Project, Costa Mesa, CA.

Hawley, R. J., Bledsoe, B. P., Stein, E. D., & Haines, B. E. (2012). Channel Evolution Model of Semiarid Stream Response to Urban Induced Hydromodification1. JAWRA Journal of the American Water Resources Association, 48(4), 722-744.

NETR Online http://www.historicaerials.com

USGS 2014 http://water.usgs.gov/osw/streamstats

Figure Set 1. DH-1, Otay Village

1953 – Watershed dominated by grazed land and scrub vegetation.

2002 - Pre-Otay Fire

2003 - Post-Otay Fire. Fire impact was greatest in the lower watershed.

2013 – Scrub vegetation has recovered from the Otay Fire.

Figure Set 2. DH-2, Bear Valley

1893 – Approximate watershed boundary. One road traverses the watershed (Bear Valley).

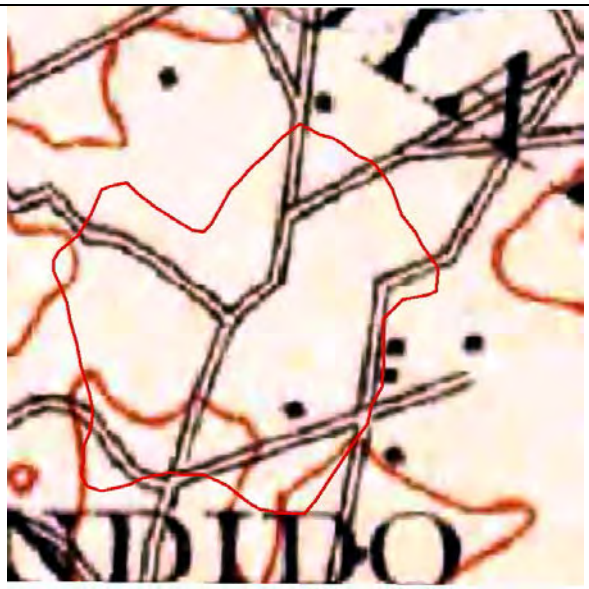

1901 – Road network expands to serve orchards and other agricultural fields.

1947 – Dominant land use is orchards.

1964 – Suburban development expands into the watershed. Portions of the creek are channelized or culverted for stormwater conveyance.

1980 – Continued suburbanization of the watershed.

2003 – Additional infill on the east side of watershed.

1995 – An isolated riparian area forms downstream of the monitoring site (foreground).

2013 – The creek is channelized upstream of monitoring site. Growth of riparian area downstream.

Figure Set 3. DH-3, MDS Development

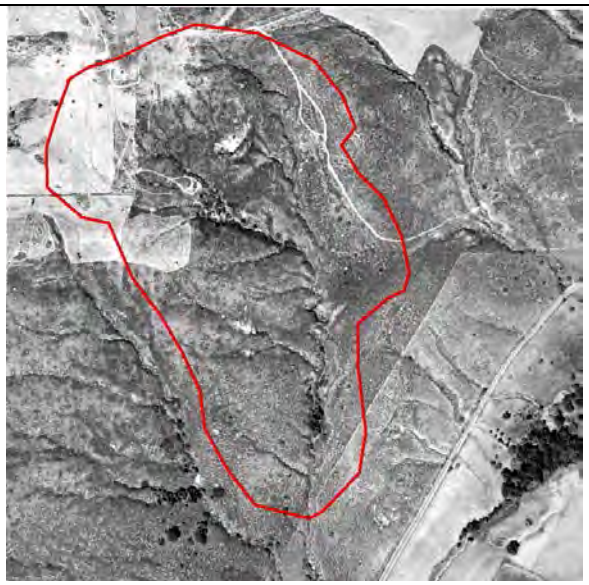

1953 – Watershed is largely undeveloped with some agricultural land use in upper watershed.

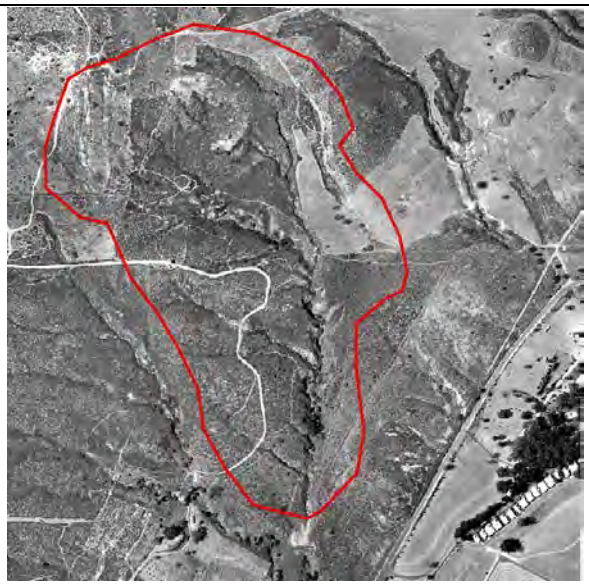

1971 – Additional land is cleared for agriculture and the road network is expanded.

1989 – Additional access roads are built in the upper watershed, and orchards become the dominant land use.

2005 – Low density development expands into the upper watershed, and the majority of orchards have gone fallow.

2005 – Sediment deposition in the lower watershed after a large storm event.

2006 – Flushing of sediment and partial revegetation of floodplain.

2010 – Narrowing of the creek and vegetation growth near the monitoring site.

2012 – Continued narrowing of the creek and revegetation of floodplain.

Figure Set 4. RM-1, Deer Valley

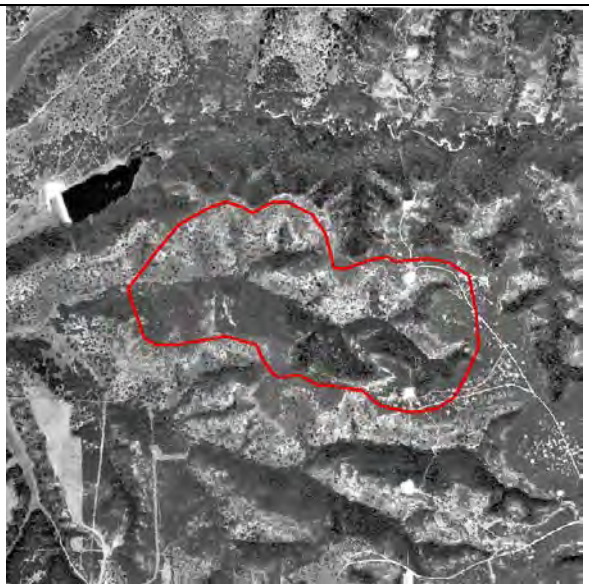

1953 – Undeveloped watershed with one trail along the upper watershed divide.

2005 – Watershed remains undeveloped. Development begins south of the watershed.

2009 – Trail network is expanded through the open space preserve.

2014 – Medium-density development expands south of the watershed.

Figure Set 5. RM-2, Sycamore Canyon

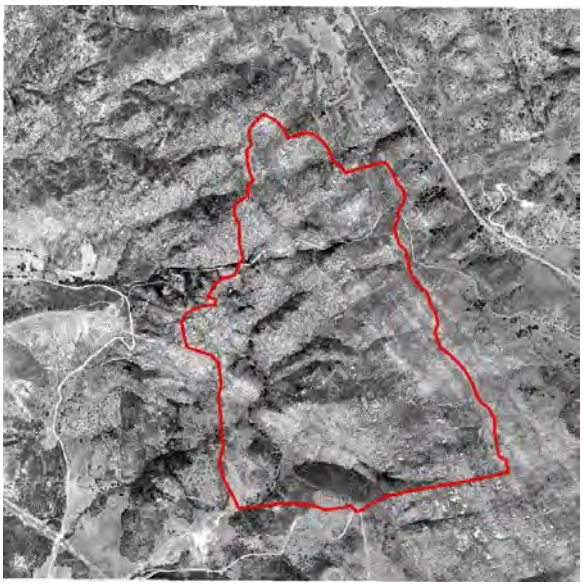

1953 – The watershed is undeveloped and dominated by scrub and grazed areas.

2003 – The only development in the watershed is a public access road, which leads to a staging area and trailhead for the open space.

2002 – Prior to the Cedar Fire of 2003 the creek was surrounded by dense scrub vegetation.

2004 – The Cedar Fire burned much of vegetation and creek began to fill with fine sediment.

2005 – Floods have flushed fine sediment from the upper watershed, widening the channel and filling the downstream stock pond.

2006 – Sediment is flushed downstream and upland vegetation begins to reestablish the valley hillslopes.

2008 – The channel begins to narrow as vegetation establishes along the floodplain.

2010 – Subsequent storms have flushed more sediment downstream.

Figure Set 6. RH-1, Ramona Grasslands

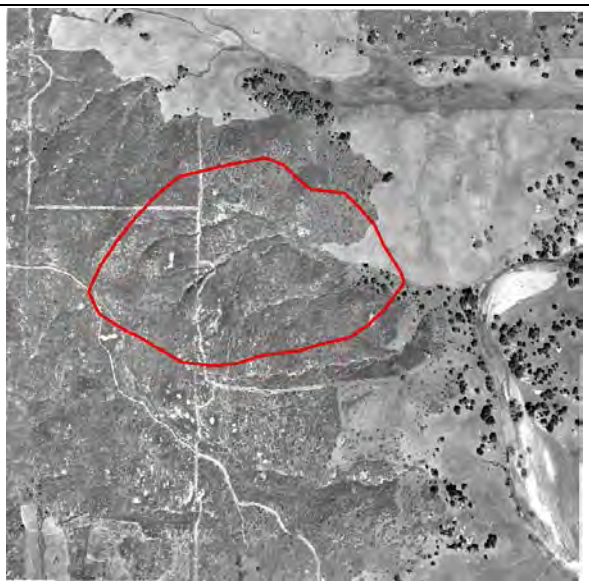

1953 – The undeveloped watershed is a mix of scrub-oak savannah and grasslands. Grazing is the dominant land use.

2003 – A portion of the upper watershed is converted to orchards, vineyards, and single family homes. Grazing continues.

2006 – Contibuting watershed before the Witch Creek Fire of 2007.

2008 – Much of the watershed was burned during the Witch Creek Fire. Channels may have incised.

2009 – Scrub vegetation begins to recover from the Witch Creek Fire.

2013 – Continued vegetation recovery.

Figure Set 7. RH-2, Schoolhouse Canyon

1953 – The watershed is undeveloped and dominated by scrub and rocky outcrops.

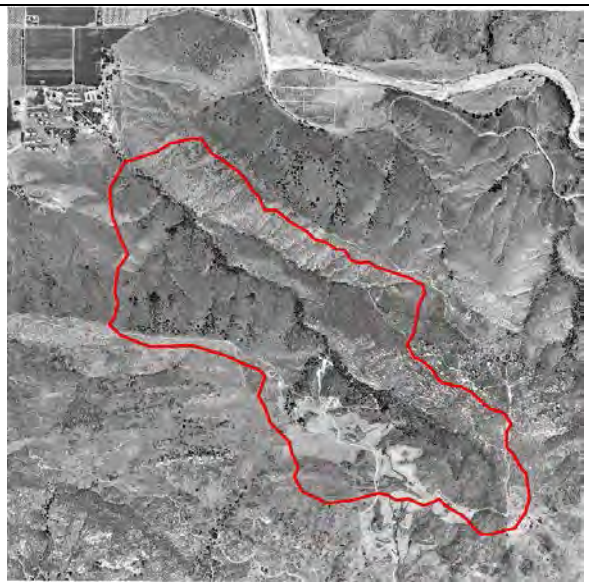

1971 – Additional roads are cut and small lots are cleared in the upper watershed.

1989 – A road network is extended into the upper watershed for future development.

1994 – Land clearing expands into the upper watershed and along the divide.

2003 – Additional lots are cleared for low density residential development.

2006 – Several single-family homes are built in the upper watershed.

2008 – The Witch Creek Fire of 2007 burned much of the upper watershed and contributed to heavy sediment deposition downstream

2013 – Vegetation has recovered from the Witch Creek Fire and houses have been rebuilt in the upper watershed.

2006 – Prior to the Witch Creek Fire, thick vegetation covered the southern valley wall and the channel corridor near the monitoring site.

2008 – The vast majority of vegetation was burned during the Witch Creek Fire, and eroded sediments deposit in the channel near the monitoring site.

2010 – Heavy deposition and channel widening near the montitoring site. Limited regrowth of riparian vegetation and upland scrub.

2013 – Vegetation has continued to recover and the channel has narrowed. Sediment is still being flushed from the watershed.

Figure Set 8. UM-1, Flanders Canyon

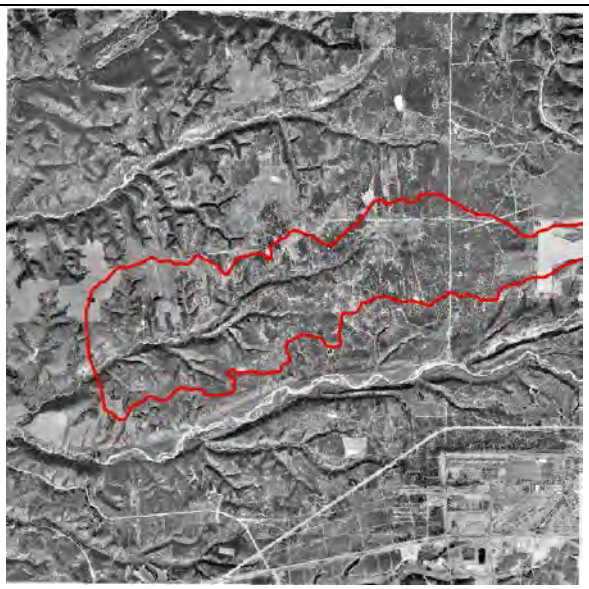

1953 – The watershed is primarily undeveloped. Primary land use is ranchland.

1980 – The majority of the upper watershed has been culverted, filled, and developed.

2005 – Development expands into the lower watershed and overall urban density increases.

2013 – The most recent aerial image shows no change in land use since 2005.

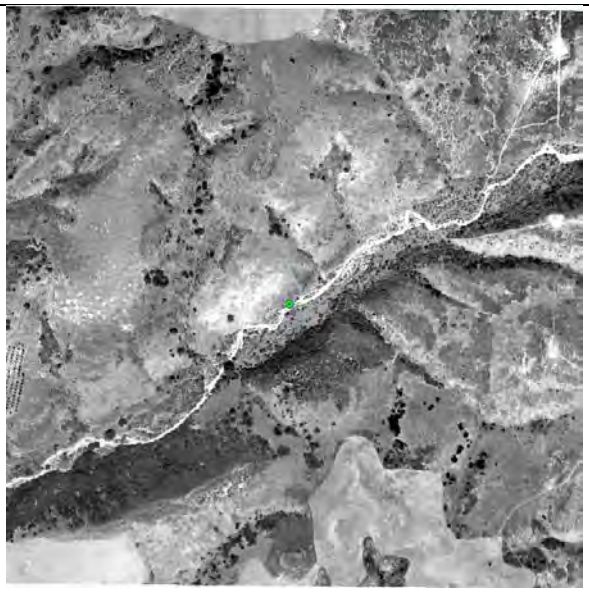

1953 – The earliest aerial photos show the creek as an ephemeral, primarily single-thread channel.

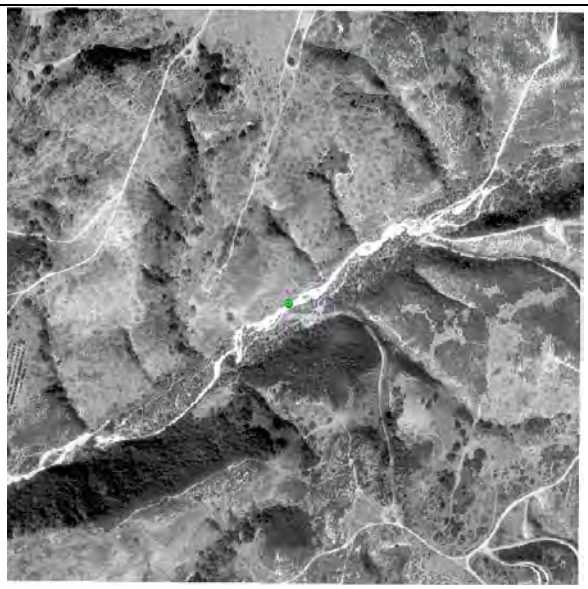

1980 – The creek has widened in response to hydromodification in the upper watershed.

1989 – Grading associated with the construction of Camino Santa Fe and development projects has directly modified the creek and watershed.

1994 – The creek has doubled in width since the 1980 aerial images were taken. Development continues on adjacent hillslopes.

2002 - Continued sediment deposition in the channel near the monitoring site.

2003 – The channel narrows as a low flow channel develops and the floodplain is revegetated.

2006 – Continued channel narrowing after completion of the Camino Santa Fe and a large development project (bottom right).

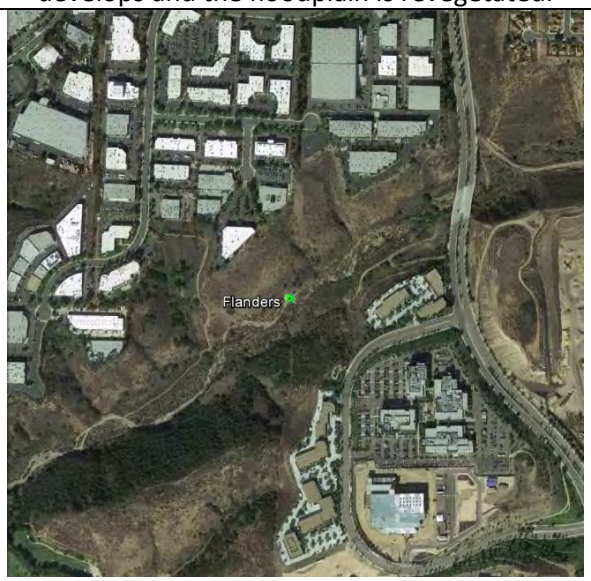

2014 – Today the creek alternates between reaches of well-connected channel and floodplain, and small braids with vegetated bars.

Figure Set 9. UH-1, Saratoga

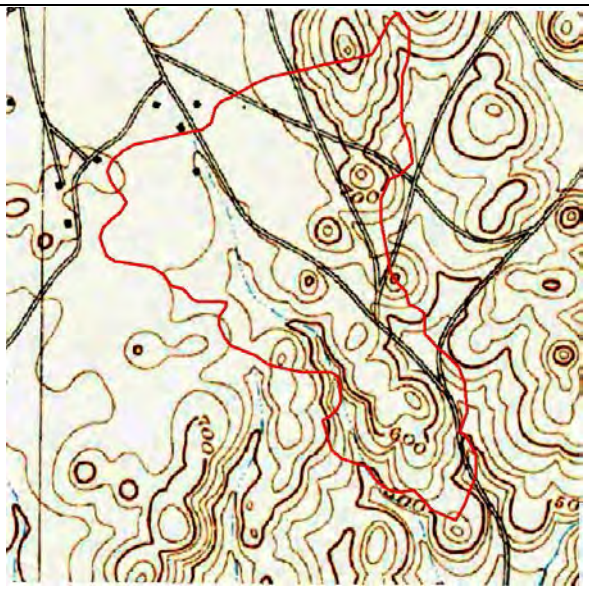

1893 – An early road system and off-site evidence of ranching exists. The map shows an ephemeral channel. Watershed boundary is skewed right.

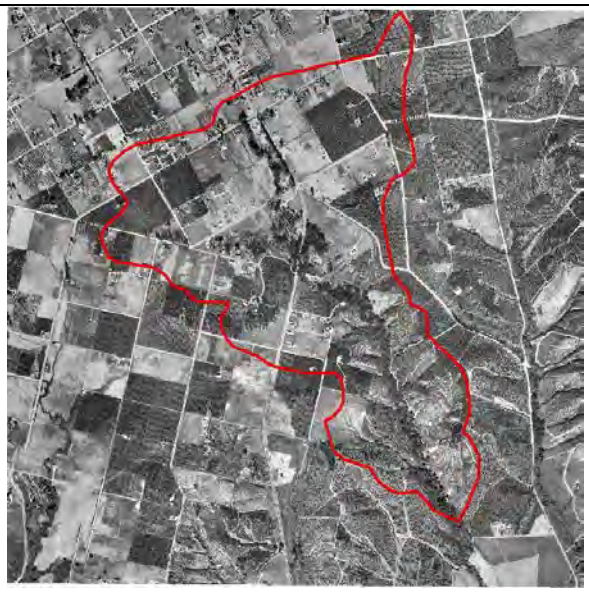

1947 - A field and road system spreads into the watershed after World War II. The channel corridor is heavily vegetated.

1964 - The headwaters start to develop, and isolated houses start to appear along roads elsewhere in the watershed.

1989 – Significant urbanization occurs in the upper watershed and lower density development occurs close to the channel in the lower watershed.

2002 - The watershed approaches full build-out except for the riparian corridor.

2014 – The watershed remains the same since the 2002 aerial imagery.